Calculation and analysis of NMR spin–spin coupling constants

Dieter Cremer[a] and Jürgen Gräfenstein[b]

Received 16th January 2007, Accepted 13th February 2007
First published as an Advance Article on the web 20th March 2007
DOI: 10.1039/b700737j

The analysis of NMR spin–spin coupling leads to a unique insight into the electronic structure of closed-shell molecules, provided one is able to decode the different features of the spin–spin coupling mechanism. For this purpose, the physics of spin–spin coupling is described and the way how spin–spin coupling constants (SSCCs) can be quantum mechanically determined. Based on this insight, a set of requirements is derived that guide the development of a quantum mechanical analysis of spin–spin coupling. It is demonstrated that the J-**OC**-PSP (= J-OC-OC-PSP: Decomposition of *J* into orbital contributions using orbital currents and partial spin polarization) analysis method fulfills all requirements. J-**OC**-PSP makes it possible to partition the isotropic indirect SSCC *J* or its reduced analogue *K* as well as the four Ramsey terms (Fermi contact (FC), spin dipole (SD), diamagnetic spin orbit (DSO), paramagnetic spin orbit (PSO)) leading to *J* (or *K*) into Cartesian components (for the anisotropic Ramsey terms SD, DSO, PSO), orbital contributions or electron interaction terms. For the purpose of decoding the spin–spin coupling mechanism, FC, SD, DSO, and PSO coupling is discussed in detail and related to electronic and bonding features of the molecules in question. The myth of empirical and semiempirical relationships between SSCCs and bonding features is unveiled. It is found that most relationships are only of limited, partly dubious value, often arising from a fortuitous cancellation of terms that cannot be expected in general. These relationships are replaced by quantum chemical relations and descriptions that directly reflect the complex electronic processes leading to spin–spin coupling.

1. Introduction

When a new chemical compound is synthesized, one of the first investigations to be carried out will be the measurement of the nuclear magnetic resonance (NMR) spectrum. Because of the sensitivity of NMR parameters such as NMR chemical shifts or spin–spin coupling constants (SSCC) to structural and conformational features of a molecule, NMR spectral data provides in a relatively easy way useful information on the identity and the structure of the new compound.[1–15] There exist in most cases sufficient reference data that makes a qualitative structure determination or verification possible.[16–19] Only after these first NMR investigations have been done, is it normally decided whether a direct structure determination with other methods such as X-ray, electron diffraction or microwave spectroscopy should be performed or whether a detailed spectroscopic, thermochemical, *etc*. characterization is desirable. However, all these additional investigations require in most cases much more time and efforts than the NMR measurements and, therefore, they are only done for interesting compounds. This is the reason why for many compounds, there is just an NMR spectrum available that has to provide all the information and insights an experimentalist wants to have on a new compound.

The information content of an NMR spectrum can be extended and completed with the help of quantum chemical calculations of NMR parameters.[20–22] This is best done when for some appropriate trial structure NMR chemical shifts and spin–spin coupling constants (SSCCs) are calculated and compared with the existing NMR data. If the two sets of NMR data agree, the compound in question is most likely to possess the molecular structure used in the calculation and, therefore, is positively identified. All molecular properties determined in the calculation can be assigned to the new compound and, accordingly, the experimentalist gets a detailed description of the compound in question. If the quantum chemical description of the molecule can be obtained in a faster and more economical way than additional experimental investigations, an ideal basis for the collaboration between experimentalists and quantum chemists will exist.

The importance of calculating NMR parameters was early recognized, however it took till the 1980s before reliable quantum chemical programs for the routine calculation of NMR magnetic shieldings and chemical shifts became available. The calculation of magnetic shieldings is described in several review articles[23–27] and is not the subject of this article. Equally or even more important for structure elucidation *via* NMR spectroscopy are SSCCs, either measured or calculated ones.[28–32] Value and sign of a SSCC are directly related to the pattern of bonds connecting the coupling nuclei and therefore a manifold of relationships between structural and conformational features of a molecule and its SSCCs have been established in the last five decades.[1–15,28–32] Best known is the

[a] *Department of Chemistry and Department of Physics, University of the Pacific, 3601 Pacific Avenue, Stockton, California 95211, USA*
[b] *Department of Theoretical Chemistry, Göteborg University, Reutersgatan 2, S-41320 Göteborg, Sweden*

Karplus relationship,[33–35] which relates the value of a vicinal SSCC $^3J(A,D)$ between nuclei A and D in a molecular fragment $A–B–C–D$ to the dihedral angle $\tau(A–B–C–D)$. Detailed summaries and extensive discussions on the various structural relationships based on SSCC have been given among others by Contreras and co-workers[30–32] (see also articles in ref. 15 and summaries in ref. 7 and 11–14).

Clearly, quantum chemical calculations of SSCCs can substantially aid the understanding of the spin–spin coupling mechanism and thereby increase the value of SSCCs as structural and conformational descriptors of molecules. Quantum chemistry can advance the analysis of SSCCs to a point that the information content of SSCCs also with regard to the electronic structure of a molecule becomes accessible. The SSCC between two nuclei depends on the distribution of electrons in a bond or a chain of bonds connecting these nuclei and, therefore, it indirectly describes the bonding situation of the molecule under investigation.

There have been many attempts to relate the SSCC to the electronic structure of a molecule, where in the beginning these attempts were limited to qualitative considerations. Early work considered excitation patterns, the nodal topology of the orbitals involved or orbital through-space overlap.[36,37] More advanced work tried to rationalize the coupling mechanism by decomposing it into orbital contributions[38,39] where special interest was given to the core orbital contributions[40] or the indirect contributions of the π-orbitals.[41–44] Contreras and co-workers used localized orbitals and a polarization propagator approach to identify orbital contributions important for a given spin–spin coupling mechanism such as through-bond or through-space.[45–48] More recently, localized natural bond orbitals (NBOs) have been used by Contreras[49,50] for an analysis of SSCCs. Their NJC (natural J-coupling) analysis[49] was later applied in similar or in modified form by others (see also ref. 32).[51,52] Lazzeretti[53] developed a local analysis of the spin–spin coupling mechanism based on current and energy densities. In this connection, investigations should be mentioned that split up SSCCs into different path contributions in those cases where the topology of the molecular bonding framework offers different coupling paths.[54–57] These studies did not directly relate to the electronic structure of a molecule, however they were essential for the analysis of spin–spin coupling insofar as they showed (although never mentioned in this form) that spin–spin coupling in general is not bound to just one coupling path.

The majority of all attempts to analyze the spin–spin coupling mechanism has focused on the FC term. Early work in this direction was also hampered by the fact that unreliable or incomplete theory had to be used to calculate SSCCs. In none of these investigations, a global, unified approach to the problem was presented. Emphasis was always laid on special aspects of spin–spin coupling interesting for a given problem considered.

With the routine calculation of fairly accurate SSCCs based on density functional theory (DFT),[58] (for later developments see ref. 59 and 60) there is for the first time the possibility of assessing electronic structure features in a systematic way directly from routinely computed SSCCs. For this purpose, we developed the J-**OC**-PSP (= J–OC–OC–PSP: decomposition of J into orbital contributions using orbital currents and partial spin polarization) method in recent years and applied it to a variety of SSCC problems.[61–74] J-**OC**-PSP is based on a decomposition of the SSCC into one-, two-, and n-orbital contributions.[61,62] It can be applied to all four Ramsey contributions[75] of the coupling mechanism, namely the Fermi contact (FC),[61,62] spin dipole (SD),[63] paramagnetic spin–orbit (PSO), and the diamagnetic spin orbit (DSO) part[64,65] where one distinguishes between one- and two-electron interactions.[69] Results of the analysis are presented in terms of spin density, orbital current, and energy density distributions.[61–65,68] This helps to understand which orbitals are actively or just passively transferring spin information between the coupling nuclei.[62] Using localized molecular orbitals (LMOs) as suitable descriptive tools, one can study the contribution of the bond LMOs in dependence of atom electronegativity and bond polarizability,[61,70] the influence of lone pair LMOs on the coupling mechanism,[61,70] the passive but nevertheless important role of π-orbitals for spin transport,[62,65,66] the description of multiple bonding and π-delocalization by the non-contact terms,[66,67] or rear lobe interactions of bond LMOs in saturated molecules.[68] Also, general mechanistic features such as through-bond and through-space coupling,[68,73] across-H-bond coupling,[71,72] long range coupling,[66] and multipath coupling[74] can be efficiently analyzed in this way.

In the following we will discuss the quantum mechanical basis of the spin–spin coupling mechanism and the calculation of SSCC with the help of DFT (section 2). In section 3, previous efforts of relating SSCCs to the electronic structure of a molecule, especially its bonding features will be summarized. Section 4 is devoted to the description of J-**OC**-PSP method where its characterization in more general terms, its relation to the physical mechanism of spin–spin coupling, and its applicability is at the focus rather than a detailed derivation of its mathematical and quantum mechanical basis. Finally, in section 5, we will discuss some selected SSCC problems to demonstrate the superiority of J-**OC**-PSP compared to other methods.

2. Theory of NMR spin–spin coupling constants

The appearance of an NMR spectrum is determined by the magnetic shielding values of the nuclei in a molecule and the SSCCs between these nuclei. Therefore it is useful to include both parameters in the theoretical treatment with the goal of focusing later just on a special set of SSCCs, namely the isotropic indirect SSCCs. The theory of NMR spin–spin coupling constants (SSCCs) can be sketched in seven steps.

(1) Explanation of the measured NMR spectrum with the help of an effective spin-Hamiltonian.

(2) Expression of the energy of a closed shell molecule in the presence of an external homogeneous magnetic field and the magnetic field of the nuclei of the molecule. This can be best done utilizing perturbation theory where the terms of the perturbation expansion can be identified using the effective spin-Hamiltonian from (1).

(3) NMR shieldings and SSCCs result as second derivatives of the electronic energy with regard to the external magnetic

field and the magnetic field of the nuclei. General formulae for the second derivatives can be found with the help of non-degenerate time-independent perturbation theory.[75]

(4) Development of the electronic molecular Hamiltonian considering its dependence on the magnetic induction $\boldsymbol{B}$ caused by an external field and on the nuclear magnetic moments $\boldsymbol{M}_N$ where N denotes nuclei A, B, *etc*.

(5) Determination of the derivatives needed in (3) for calculating the SSCC using the electronic molecular Hamiltonian from (4).

(6) Analysis of the operator derivatives required for the calculation of the indirect isotropic SSCC.

(7) Use of DFT to calculate the indirect isotropic SSCC.

When outlining the theory we will apply the following conventions: The perturbing nucleus will be denoted by (B) and the responding nucleus by (A). The spin moment of nucleus (B) will always be α, that of nucleus (A) always β. The spin polarization terms will be described using either spin orbitals $\psi_{k\sigma}$ (σ: spin index) or space orbitals ϕ_k. Unperturbed orbitals will be denoted with the superscript (0), the first-order perturbed orbitals with a superscript of the form (B), X where X = FC, SD, or PSO. The same superscript will be used for the resulting spin polarization and current densities. The use of space orbitals is possible because only closed-shell systems are considered and accordingly the magnetic perturbations cause either identical (PSO) or opposite (FC,SD) first-order space orbitals for a pair of spin orbitals ($\psi_{k\alpha}$, $\psi_{k\beta}$). For the spin orbit terms space orbitals ϕ_k are considered exclusively. We will use indices *i, j* for electrons and (equivalently) occupied spin orbitals, *k, l, m*,... for occupied space orbitals, indices *a, b*,... for virtual (unoccupied) spin or space orbitals, and indices *p, q*,... for general spin or space orbitals. Occupied orbitals are assumed to be localized, *i.e*. LMOs, and, unless otherwise stated, virtual orbitals to be canonical, *i.e*. CMOs. The Dirac (bra-ket) notation will be applied for orbitals. However, when no misunderstandings are possible, orbitals are simply denoted by their index for brevity. Cartesian coordinates are labeled with κ, λ.

2.1 Explanation of the measured NMR spectrum

NMR spectroscopy measures the transitions between the eigenstates of the nuclear spin system of a closed-shell molecule when exposed to an external homogeneous magnetic field. The eigenstates reflect the interactions between magnetic nuclei and external field modified by a direct (through-space) dipolar coupling between the nuclei and an indirect coupling mediated by the electrons of the closed-shell molecule. A given nucleus leads to an NMR signal provided it possesses a non-zero magnetic dipole moment $\vec{\mu}_A$

$$\vec{\mu}_A = \hbar\gamma_A \boldsymbol{I}_A \tag{1}$$

where γ_A is the magnetogyric ratio, and $\boldsymbol{I}_A$ the spin angular momentum (in units of $\hbar$) of nucleus A. The fact that each nucleus of a molecule is surrounded by electrons which interact *via* their spin magnetic moment or their orbital angular moment with the magnetic moments of the nuclei, has two consequences: (i) the electrons screen each nucleus magnetically as reflected by the nuclear magnetic shielding tensor $\underline{\underline{\sigma}}_A$ where the degree of shielding is directly reflected by the position of the NMR signal of a given nucleus. (ii) Beside the direct spin–spin coupling between the magnetic moments $\vec{\mu}_A$ and μ_B as described by the classical dipolar coupling tensor $\underline{\underline{D}}_{AB}$

$$\underline{\underline{D}}_{AB} = \frac{\mu_0}{4\pi}\frac{3\boldsymbol{R}_{AB}\boldsymbol{R}_{AB} - \underline{\underline{I}}\boldsymbol{R}_{AB}^2}{R_{AB}^5} \tag{2}$$

(μ_0 is the Bohr magneton and $\boldsymbol{R}_{AB} = \boldsymbol{R}_B - \boldsymbol{R}_A$), there is also the indirect coupling mediated by the electrons and described by the indirect spin–spin coupling tensor $\underline{\underline{J}}_{AB}$. The coupling tensor $\underline{\underline{J}}_{AB}$ represents or leads to the coupling properties measured in a NMR experiment. In theory however, it is more useful to work with the reduced spin–spin coupling tensor $\underline{\underline{K}}_{AB}$, which is related to $\underline{\underline{J}}_{AB}$ *via* eqn (3)

$$\underline{\underline{J}}_{AB} = h\frac{\gamma_A}{2\pi}\frac{\gamma_B}{2\pi}\underline{\underline{K}}_{AB} \tag{3}$$

The value of the reduced spin–spin coupling tensor reflects directly the impact of the electrons on spin–spin coupling whereas the elements of the tensor $\underline{\underline{J}}_{AB}$ are scaled by the magnetogyric ratios γ of the coupling nuclei A and B. The larger γ_A is the larger is the sensitivity of nucleus A and the larger becomes the spin–spin coupling of A with other nuclei, which for a NMR spectroscopist is of considerable relevance when measuring NMR spectra. Since values of γ are well-known for all common nuclei of the periodic table,[2,15,76] the analysis of spin–spin coupling is better done for reduced spin–spin coupling (tensor $\underline{\underline{K}}_{AB}$ and isotropic reduced coupling constant K_{AB}^{iso}, see below). In the present paper, all values of spin–spin coupling constants are given for the isotopes ^{1}H, ^{13}C, and ^{19}F.

Considering just magnetic shielding and spin–spin coupling, a relatively simple effective spin-Hamiltonian can be formulated where the term effective indicates that the electronic degrees of freedom have been eliminated from the Hamiltonian and condensed into a number of parameters. The effective spin-Hamiltonian accounts for the major features of an NMR spectrum, namely the position of the signals of the various magnetic nuclei of a molecule as determined by nuclear magnetic shielding tensors and the splitting of the signals as caused by spin–spin interactions of the magnetic nuclei,[2] as it is observed when an external homogeneous magnetic field $\boldsymbol{B}_0$ is applied:

$$\hat{H} = -\sum_A B_0^{\dagger}(1 - \underline{\underline{\sigma}}_A)\vec{\mu}_A + \frac{1}{2}\sum_{A,B\neq A}\vec{\mu}_A^{\dagger}(\underline{\underline{D}}_{AB} + \underline{\underline{K}}_{AB})\vec{\mu}_B \tag{4}$$

Hamiltonian (4) can be used to calculate the features of an NMR spectrum, however it does not provide any insight into the relationship between electronic structure of the molecule and the NMR parameters since it generates the energy eigenstates of the nuclear spin system without any reference to the indirect spin–spin coupling mechanism as transported by the electrons of the molecule.

In the gas, liquid phase or any solution phase, molecules rapidly tumble and therefore rotational averages of the second rank tensors $\underline{\underline{\sigma}}_A$, $\underline{\underline{D}}_{AB}$, and $\underline{\underline{K}}_{AB}$ have to be taken. Contrary to $\underline{\underline{\sigma}}_A$ and $\underline{\underline{K}}_{AB}$, the direct coupling tensor $\underline{\underline{D}}_{AB}$ is a traceless tensor so that its rotational average vanishes, *i.e*. the direct

coupling between nuclei A and B of the tumbling molecule vanishes. Hence, the NMR spectrum of the molecule is determined by just the isotropic magnetic shielding constants σ_A^{iso} and the isotropic reduced spin–spin coupling constants K_B^{iso}. The averaged (isotropic) effective spin-Hamiltonian for a uniform magnetic field parallel to the z-axis takes the form

$$\hat{H}^{\mathrm{iso}} = -\sum_A (1-\sigma_A^{\mathrm{iso}}) B_0 \mu_{A,z} + \frac{1}{2}\sum_{A,B\neq A} K_{AB}^{\mathrm{iso}}\, \vec{\mu}_A \cdot \vec{\mu}_B \qquad (5)$$

where

$$\sigma_A^{\mathrm{iso}} = \frac{1}{3}\mathrm{Tr}\,\underline{\underline{\sigma}}_A = \frac{1}{3}(\sigma_A^{xx}+\sigma_A^{yy}+\sigma_A^{zz}) \qquad (6)$$

and

$$K_{AB}^{\mathrm{iso}} = \frac{1}{3}\mathrm{Tr}\,\underline{\underline{K}}_{AB} = \frac{1}{3}(K_{AB}^{xx}+K_{AB}^{yy}+K_{AB}^{zz}) \qquad (7)$$

In the following, the superscript iso will be suppressed for reasons of brevity.

2.2 The energy of a molecule in the presence of magnetic perturbations

The nuclear magnetic excitations and the electronic excitation in a molecule proceed at rather different energy scales (for example, changes in the nuclear energy level of ^{1}H at 400 MHz are just of the order of 10^{-5} kcal mol^{-1}). Owing to this fact, one can determine the parameters σ_A and $\underline{\underline{K}}_{AB}$ in eqns (4) and (5) by adapting the Born–Oppenheimer approximation to the nuclear magnetic moments (rather than the nuclear coordinates). That means that one replaces the operators $\hat{\vec{\mu}}_A$ in eqns (4) and (5) by classical vector quantities $\vec{\mu}_A$. Then, the total energy of the molecule can be written as a function of the $\vec{\mu}_A$ and the external magnetic field $\boldsymbol{B}_0$.

Generally, the energy $E^{(0)}$ of a molecule changes under the impact of a (vector) perturbation $\boldsymbol{u}$ according to eqn (8)

$$E(\boldsymbol{u}) = E^{(0)} + \boldsymbol{E}^{(1)}\boldsymbol{u} + \frac{1}{2}\boldsymbol{u}^{\dagger}\underline{\underline{E}}^{(2)}\boldsymbol{u} + \cdots \qquad (8)$$

which represents the Taylor series expansion of E at the reference point $\boldsymbol{u} = 0$. In eqn (8), $\boldsymbol{E}^{(1)}$, $\underline{\underline{E}}^{(2)}$,$\cdots$ are vector, second-rank tensor, (higher rank tensor) quantities that represent molecular properties and measure the response of the molecule to the perturbation $\boldsymbol{u}$. Eqn (8) will hold if the perturbation $\boldsymbol{u}$ is sufficiently small compared to the electronic excitation energies of the molecule. Considering that this holds when the perturbation is caused by a homogeneous external field and the field of the magnetic nuclei of a closed-shell molecule, eqn (8) can be written down for the situation of the NMR experiment carried out under idealized conditions (see below).

$$E(\boldsymbol{B}_0,\vec{\mu}) = E^{(0)} + \frac{1}{2}\boldsymbol{B}_0^{\dagger}\underline{\underline{E}}^{(20)}\boldsymbol{B}_0 + \sum_A \boldsymbol{B}_0^{\dagger}\underline{\underline{E}}^{(11)}\vec{\mu}_A + \frac{1}{2}\sum_{A,B\neq A}\vec{\mu}_A^{\dagger}\underline{\underline{E}}_{A,B}^{(02)}\vec{\mu}_B \qquad (9)$$

In eqn (9) it is already considered that first order properties $\underline{\underline{E}}^{(10)}$ and $\underline{\underline{E}}^{(01)}$ do not appear for a closed-shell molecule (they correspond to the g value and the hyperfine structure constant in EPR spectroscopy[77]) and that the third order properties are too small to be of any relevance. Actually, third-order quantities are by the order of α^2 ($\alpha \approx 1/137.04\ldots$ Sommerfeld fine structure constant) *i.e.*, by about a factor of 10^{-4} smaller than second-order quantities, which means that they are below the resolution of the experimental methods available.

Tensor $\underline{\underline{E}}^{(20)}$ corresponds to the molecular magnetizability, which is obtained by taking the total energy derivative with regard to the external magnetic field (or better: magnetic induction) at zero field strength and zero magnetic moments:

$$\underline{\underline{E}}^{(20)} = \left.\frac{\mathrm{d}^2 E(\boldsymbol{B}_0,\vec{\mu})}{\mathrm{d}\boldsymbol{B}_0^2}\right|_{\boldsymbol{B}_0=0,\vec{\mu}=0} \qquad (10)$$

for all $\vec{\mu}$. Since the molecular magnetizability does not influence the NMR spectrum it will be discarded in the following. The other two terms of eqn (9) can be readily identified by relating them to the effective spin-Hamiltonian (4). The second order cross term $\underline{\underline{E}}^{(11)}$ is obtained by deriving the electronic molecular energy with regard to the magnetic induction $\boldsymbol{B}_0$ and the nuclear magnetic moment $\vec{\mu}_A$ of nucleus A; it represents the nuclear magnetic shielding tensor $\underline{\underline{\sigma}}_A$ corrected by a constant.

$$\underline{\underline{E}}^{(11)} = \left.\frac{\mathrm{d}^2 E(\boldsymbol{B}_0,\vec{\mu})}{\mathrm{d}\boldsymbol{B}_0\,\mathrm{d}\vec{\mu}_A}\right|_{\boldsymbol{B}_0=0,\vec{\mu}=0} = \underline{\underline{\sigma}}_A - 1 \qquad (11)$$

Similarly, the tensor $\boldsymbol{E}^{(02)}$ is found to be

$$\underline{\underline{E}}^{(02)} = \left.\frac{\mathrm{d}^2 E(\boldsymbol{B}_0,\vec{\mu})}{\mathrm{d}\vec{\mu}_A\,\mathrm{d}\vec{\mu}_B}\right|_{\boldsymbol{B}_0=0,\vec{\mu}=0} = \underline{\underline{D}}_{AB} + \underline{\underline{K}}_{AB}. \qquad (12)$$

i.e. equal to the total spin–spin coupling tensor between nuclei A and B. As mentioned earlier in this section, $\underline{\underline{D}}_{AB}$ does not contribute to the isotropic limit of $\underline{\underline{E}}^{(02)}$, *i.e.*, only $\underline{\underline{K}}_{AB}$ is needed to determine isotropic SSCCs.

2.3 Calculation of second order properties by perturbation theory

Nondegenerate time-independent perturbation theory leads to eqn (13) in the case of a second order property measured as response of a molecule to a perturbation $\boldsymbol{u}$:

$$\frac{\mathrm{d}^2 E(\boldsymbol{u})}{\mathrm{d}u_\kappa\,\mathrm{d}u_\lambda} = \left\langle \Psi_0 \left| \frac{\mathrm{d}^2\hat{H}}{\mathrm{d}u_\kappa\,\mathrm{d}u_\lambda}\right|\Psi_0\right\rangle - 2\sum_{n>0}(E_n-E_0)^{-1} \times \left\langle \Psi_0\left|\frac{\mathrm{d}\hat{H}}{\mathrm{d}u_\kappa}\right|\Psi_n\right\rangle\left\langle \Psi_n\left|\frac{\mathrm{d}\hat{H}}{\mathrm{d}u_\lambda}\right|\Psi_0\right\rangle \qquad (13)$$

For the first term, just the ground state wave function Ψ_0 is needed whereas for the second term the excited state wave functions Ψ_n with associated state energies E_n are required. In the case of the reduced indirect spin–spin coupling tensor $\boldsymbol{K}_{AB}$ one obtains:

$$K_{AB}^{\kappa\lambda} = \frac{\mathrm{d}^2 E(\vec{\mu})}{\mathrm{d}\mu_A^\kappa\,\mathrm{d}\mu_B^\lambda} = \left\langle \Psi_0 \left| \frac{\mathrm{d}^2\hat{H}}{\mathrm{d}\mu_A^\kappa\,\mathrm{d}\mu_B^\lambda}\right|\Psi_0\right\rangle - 2\sum_{n>0}(E_n-E_0)^{-1} \times \left\langle \Psi_0\left|\frac{\mathrm{d}\hat{H}}{\mathrm{d}\mu_A^\kappa}\right|\Psi_n\right\rangle\left\langle \Psi_n\left|\frac{\mathrm{d}\hat{H}}{\mathrm{d}\mu_B^\lambda}\right|\Psi_0\right\rangle \qquad (14)$$

where κ and λ define Cartesian coordinates x, y, z and the derivatives are determined for zero nuclear magnetic moments. For the purpose of evaluating the spin–spin coupling constants one has to take the first and second derivative of the Hamiltonian with regard to the Cartesian components (κ, λ = x, y, z) of the nuclear magnetic moments $\vec{\mu}$ of the coupling nuclei. The first second-order term corresponds to an expectation value over the ground state wave function whereas the second term is a sum-over-states (SOS) contribution of the excited states Ψ_n with energy E_n. Eqn (14) defines a 2-rank tensor, the elements of which will split up into at least two different contributions. In the case of the magnetic shielding tensor the first term would correspond to the diamagnetic and the second term to the paramagnetic part. However, in the case of the spin–spin coupling constants, there are actually four rather than just two contributions because of the form of the Hamiltonian and therefore one can no longer speak just of a diamagnetic and a paramagnetic part. For the purpose of identifying the various contributions to the NMR spin–spin coupling mechanism, we have to consider next the form of the electronic molecular Hamiltonian in dependence of the nuclear magnetic moments $\vec{\mu}_A$ and a uniform external magnetic field $\boldsymbol{B}_0$.

2.4 The electronic molecular Hamiltonian in a magnetic field

Without a magnetic field present, the non-relativistic electronic molecular Hamiltonian has the form

$$\hat{H}(0) = \frac{1}{2}\sum_i \boldsymbol{p}_i^2 - \sum_{iA}\frac{Z_A}{r_{iA}} + \frac{1}{2}\sum_{i\neq j}\frac{1}{r_{ij}} + \frac{1}{2}\sum_{A\neq B}\frac{Z_A Z_B}{R_{AB}} \qquad (15)$$

where $\boldsymbol{p}_i = -\mathrm{i}\nabla_i$ is the momentum operator. The magnetic field $\boldsymbol{B}(\boldsymbol{r})$ is generally derived from a vector potential $\boldsymbol{A}(\boldsymbol{r})$ by the relation

$$\boldsymbol{B}(\boldsymbol{r}) = \nabla \times \boldsymbol{A}(\boldsymbol{r}) \qquad (16)$$

In the case discussed, $\boldsymbol{B}(\boldsymbol{r})$ consists of the homogeneous external field $\boldsymbol{B}_0$ and the fields generated by the nuclear magnetic momenta $\vec{\mu}_A$:

$$\begin{aligned}\boldsymbol{B}(\boldsymbol{r}_i) &= \boldsymbol{B}_0 + \sum_A \boldsymbol{B}_A(\boldsymbol{r}_i) \\ &= \nabla \times \left(\boldsymbol{A}_0(\boldsymbol{r}_i) + \sum_A \boldsymbol{A}_A(\boldsymbol{r}_i)\right)\end{aligned} \qquad (17)$$

Because of its orbital and spin motion, an electron possesses an orbital magnetic moment $\vec{\mu}_i^l = \gamma_e \boldsymbol{l}_i$ (γ_e: magnetogyric ratio of the electron; $\boldsymbol{l}$: orbital angular momentum) and a spin magnetic moment $\vec{\mu}_i^s = -g_e\mu_B\boldsymbol{s}_i$ (g_e: g-factor of the electron; μ_B: Bohr magneton; $\boldsymbol{s}_i$: spin angular momentum of electron i). Both the orbital and the spin magnetic momentum of the electron can interact with the magnetic field, and consequently the magnetic field gives rise to two kinds of additional terms in the Hamiltonian. First, the momentum operator $\boldsymbol{p}_i = -\mathrm{i}\nabla_i$ has to be replaced by the momentum operator$\vec{\pi}_i$ of electron i in the magnetic field:

$$\vec{\pi}_i = -\mathrm{i}\nabla_i + \boldsymbol{A}(\boldsymbol{r}_i) \qquad (18)$$

Secondly, there arises an additional interaction term of the form $\sum_i \boldsymbol{B}(\boldsymbol{r}_i)\vec{\mu}_i$ in the Hamiltonian, reflecting the interaction between the spin moment $\vec{\mu}_i$ of the electron i and the external field. With these two additional terms added, the non-relativistic molecular Hamiltonian takes the form

$$\hat{H}(\boldsymbol{B}) = \hat{H}(0) - \sum_i \boldsymbol{p}_i\boldsymbol{A}(\boldsymbol{r}_i) - \sum_i \vec{\mu}_i\boldsymbol{B}(\boldsymbol{r}_i) + \frac{1}{2}\sum_i[\boldsymbol{A}(\boldsymbol{r}_i)]^2 \qquad (19)$$

Note that the direct magnetostatic interaction between the $\vec{\mu}_{A,B}$ and between $\vec{\mu}_A$ and $\boldsymbol{B}_0$ is omitted in eqn (19).

Decomposing $\boldsymbol{B}(\boldsymbol{r})$ and $\boldsymbol{A}(\boldsymbol{r})$ into its constituents and expressing $\boldsymbol{B}_{A,B}(\boldsymbol{r})$ and $\boldsymbol{A}_{A,B}(\boldsymbol{r})$ through $\vec{\mu}_{A,B}$, $\hat{H}(\boldsymbol{B})$ gets the following form:

$$\begin{aligned}\hat{H}(\boldsymbol{B}_0, \vec{\mu}_A) =& \hat{H}(0) - \sum_A \vec{\mu}_A\left(\sum_i \hat{\boldsymbol{B}}_{iA}^l + \sum_i \hat{\mathbf{B}}_{iA}^s\right) \\ &- \boldsymbol{B}_0\sum_i \mu_i^l - \boldsymbol{B}_0^\dagger\underline{\underline{\hat{\chi}}}^{\mathrm{dia}}\boldsymbol{B}_0 \\ &+ \boldsymbol{B}_0^\dagger\sum_A \underline{\underline{\hat{\sigma}}}_A^{\mathrm{dia}}\vec{\mu}_A + \frac{1}{2}\sum_{A,B\neq A}\vec{\mu}_A^\dagger\underline{\underline{\hat{K}}}_{AB}^{\mathrm{DSO}}\vec{\mu}_B.\end{aligned} \qquad (20)$$

Here, $\hat{\boldsymbol{B}}_{iA}{}^l$ and $\hat{\boldsymbol{B}}_{iA}^s$ are the operators for the magnetic fields induced by the electronic magnetic moments $\vec{\mu}_i{}^l$ and $\vec{\mu}_i^s$, respectively, at position $\boldsymbol{r}_A$; $\underline{\underline{\hat{\chi}}}^{\mathrm{dia}}$ is the operator for the diamagnetic part of the magnetizability, $\underline{\underline{\hat{\sigma}}}_A^{\mathrm{dia}}$ is the diamagnetic part of the chemical shielding for nucleus A, and $\underline{\underline{\hat{K}}}_{AB}^{\mathrm{DSO}}$ is the diamagnetic spin–orbit part of the SSCC between nuclei A and B (see next paragraph). Eqn (20) provides a basis for the extraction of the Hamiltonian derivatives needed in eqn (14).

2.5 Extracting the Hamiltonian derivatives needed to calculate the SSCC

According to eqn (14) the calculation of the SSCC requires the Hamiltonian derivatives $\mathrm{d}\hat{H}/\mathrm{d}\vec{\mu}_A$ and $\mathrm{d}^2\hat{H}/\mathrm{d}\vec{\mu}_A\,\mathrm{d}\vec{\mu}_B$. From eqn (20), one finds that

$$\frac{\mathrm{d}\hat{H}}{\mathrm{d}\vec{\mu}_A} = \sum_i \hat{\boldsymbol{B}}_i^l(\boldsymbol{r}_A) + \sum_i \hat{\boldsymbol{B}}_i^s(\boldsymbol{r}_A) \qquad (21)$$

where one has to keep in mind that the derivatives have to be taken for $\vec{\mu}_A = \vec{\mu}_B = \boldsymbol{B}_0 = 0$. According to (21) derivative $\mathrm{d}\hat{H}/\mathrm{d}\vec{\mu}_A$ is determined by the magnetic field the electrons generate at $\boldsymbol{r}_A$. The explicit expressions of $\hat{\boldsymbol{B}}_i^l$ and $\hat{\boldsymbol{B}}_i^s$ read

$$\hat{\boldsymbol{B}}_{iA}^l = \underbrace{\alpha^2\frac{\boldsymbol{r}_{iA}}{r_{iA}^3}\times\boldsymbol{p}_i}_{=\hat{\boldsymbol{B}}_{iA}^{\mathrm{PSO}}} \qquad (22)$$

$$\hat{\boldsymbol{B}}_{iA}^s = \underbrace{\alpha^2\left[\frac{3(\boldsymbol{s}_i\cdot\boldsymbol{r}_{iA})}{r_{iA}^5} - \frac{\mathbf{s}_i}{r_{iA}^3}\right]}_{=\hat{\boldsymbol{B}}_{iA}^{\mathrm{SD}}} + \underbrace{\alpha^2\frac{8\pi}{3}\delta(\boldsymbol{r}_{iA})\boldsymbol{s}_i}_{=\hat{\boldsymbol{B}}_{iA}^{\mathrm{FC}}} \qquad (23)$$

The derivative $\mathrm{d}^2\hat{H}/\mathrm{d}\vec{\mu}_A\,\mathrm{d}\vec{\mu}_B$ can be evaluated explicitly as

$$\frac{\mathrm{d}^2\hat{H}}{\mathrm{d}\vec{\mu}_A\mathrm{d}\vec{\mu}_B} = \underline{\underline{\hat{K}}}_{AB}^{\mathrm{DSO}} = \alpha^4\left(\frac{\boldsymbol{r}_{iA}}{r_{iA}^3}\frac{\boldsymbol{r}_{iB}}{r_{iB}^3}\underline{\underline{I}} - \frac{\boldsymbol{r}_{iA}}{r_{iA}^3}\frac{\boldsymbol{r}_{iB}}{r_{iB}^3}\right) \qquad (24)$$

2.6 Analysis of the operator derivatives needed for the calculation of the indirect isotropic SSCC

The four operators $\underline{\underline{\hat{K}}}_{AB}^{\mathrm{DSO}}$, $\hat{\boldsymbol{B}}_{iA}{}^{\mathrm{PSO}}$, $\hat{\boldsymbol{B}}_{iA}^{\mathrm{FC}}$, and $\hat{\boldsymbol{B}}_{iA}^{\mathrm{SD}}$ correspond to the four coupling mechanisms between the nuclear magnetic moments and the electron systems that were identified by Ramsey.[75] The first two terms are related to the orbital currents of the electron system. The DSO term describes the diamagnetic part of the electron currents, *i.e.* the part that can be ascribed to a Larmor precession of the electron system. The PSO term, in contrast, reflects the paramagnetic part of the orbital current, which can be understood as a modification of previously existing orbital currents. The vector potential for a given magnetic field is not defined unambiguously because its choice is subjected to a gauge ambiguity. Consequently, the individual values of the DSO and PSO terms depend on how the vector potential is gauged. However, the sum of the PSO and DSO terms is invariant with regard to this ambiguity.

The two terms related to $\hat{\boldsymbol{B}}_i^s(\boldsymbol{r}_A)$ describe the interaction of the electronic spin with the nuclear magnetic field. The magnetic field of the nucleus consists of two parts: an extended dipole field outside the nucleus and a strongly localized field inside the nucleus. The SD term corresponds to the dipole field, whereas the FC term describes a contact interaction between electron spin and nuclear magnetic field at the surface of the nucleus considering that the latter possesses a finite size. The total SSCC becomes

$$\begin{aligned} K_{AB}^{\kappa\lambda} = {} & \langle \Psi_0 | \hat{K}_{AB}^{\mathrm{DSO},\kappa\lambda} | \Psi_0 \rangle - 2 \sum_{n>0} (E_n - E_0)^{-1} \langle \Psi_0 | \hat{B}_A^{\mathrm{PSO},\kappa} | \Psi_n \rangle \\ & \times \langle \Psi_n | \hat{B}_B^{\mathrm{PSO},\lambda} | \Psi_0 \rangle - 2 \sum_{n>0} (E_n - E_0)^{-1} \langle \Psi_0 | \hat{B}_A^{\mathrm{SD},\kappa} + \hat{B}_A^{\mathrm{FC},\kappa} | \Psi_n \rangle \\ & \times \langle \Psi_n | \hat{B}_B^{\mathrm{SD},\lambda} + \hat{B}_B^{\mathrm{FC},\lambda} | \Psi_0 \rangle \end{aligned} \tag{25}$$

where $\hat{\boldsymbol{B}}_A^{\mathrm{PSO}} = \sum_i \hat{\boldsymbol{B}}_{iA}^{\mathrm{PSO}} etc.$ In eqn (25), it has been taken into account that terms containing products of the form $\langle \cdots \hat{\boldsymbol{B}}_A^{\mathrm{PSO}} \cdots \rangle \langle \cdots \hat{\boldsymbol{B}}_B^{\mathrm{SD,FC}} \cdots \rangle$ do not contribute to the SSCC. In the case of the isotropic average, terms of the form $\langle \cdots \hat{\boldsymbol{B}}_A^{\mathrm{SD}} \cdots \rangle \langle \cdots \hat{\boldsymbol{B}}_B^{\mathrm{FC}} \cdots \rangle$ cancel as well. Thus the final form of the isotropic SSCC is

$$K_{AB} = K_{AB}^{\mathrm{DSO}} + K_{AB}^{\mathrm{PSO}} + K_{AB}^{\mathrm{FC}} + K_{AB}^{\mathrm{SD}} \tag{26a}$$

$$K_{AB}^{\mathrm{DSO}} = \langle \Psi_0 | \hat{K}_{AB}^{\mathrm{DSO}} | \Psi_0 \rangle \tag{26b}$$

$$\begin{aligned} K_{AB}^{\mathrm{PSO}} = {} & -\frac{2}{3} \sum_{n>0} (E_n - E_0)^{-1} \\ & \times \langle \Psi_0 | \hat{\boldsymbol{B}}_A^{\mathrm{PSO}} | \Psi_n \rangle \langle \Psi_n | \hat{\boldsymbol{B}}_B^{\mathrm{PSO}} | \Psi_0 \rangle \end{aligned} \tag{26c}$$

$$\begin{aligned} K_{AB}^{\mathrm{FC}} = {} & -\frac{2}{3} \sum_{n>0} (E_n - E_0)^{-1} \\ & \times \langle \Psi_0 | \hat{\boldsymbol{B}}_A^{\mathrm{FC}} | \Psi_n \rangle \langle \Psi_n | \hat{\boldsymbol{B}}_B^{\mathrm{FC}} | \Psi_0 \rangle \end{aligned} \tag{26d}$$

$$K_{AB}^{\mathrm{SD}} = -\frac{2}{3} \sum_{n>0} (E_n - E_0)^{-1} \langle \Psi_0 | \hat{\boldsymbol{B}}_A^{\mathrm{SD}} | \Psi_n \rangle \langle \Psi_n | \hat{\boldsymbol{B}}_B^{\mathrm{SD}} | \Psi_0 \rangle \tag{26e}$$

where the factor of 1/3 results from the isotropic averaging. In summary, the isotropic SSCC consists of four terms, each of which corresponds to one of the four mechanisms for spin–spin coupling, *i.e.*, DSO, PSO, FC, and SD coupling. These four terms were identified first by Ramsey[75] and accordingly are called *Ramsey terms*.

All terms in eqn (26a)–(26e), contain either an operator connecting nuclei A and B (DSO) or one operator at nucleus A and one at nucleus B (PSO, FC, SD). This reflects the various stages of the magnetic interaction leading to nuclear spin–spin coupling: at the first stage, the magnetic field of nucleus B (*perturbing nucleus*) induces either orbital currents (DSO, PSO) or spin polarization (FC, SD) in the electron system. At the second stage, orbital currents or spin polarization mitigate through the electron system of the molecule so that at the third stage, nucleus A (*responding nucleus*) experiences an extra magnetic field. Eqn (26a)–(26e), are symmetric with respect to the two nuclei. This implies that the coupling process is invariant to an exchange of perturbing and responding nucleus.

2.7 Using DFT to calculate isotropic indirect SSCCs

In DFT, the ground-state energy is expressed as a functional of the one-electron density rather than an expectation value of the Hamiltonian formed with the ground-state function.[78,79] In the Kohn–Sham (KS) formulation of DFT,[80] the many-electron problem is mapped on a model system of non-interacting electrons moving in an effective potential, the so-called KS potential. The spin orbitals $\psi_p(\boldsymbol{r}, \sigma)$ and orbital energies ε_p for these particles are given by the KS equations

$$\hat{F}\psi_p(\boldsymbol{r}, \sigma) = \varepsilon_p \psi_p(\boldsymbol{r}, \sigma) \tag{27a}$$

$$\hat{F} = \frac{1}{2}\hat{\boldsymbol{p}}^2 + v_{KS}(\boldsymbol{r}, \sigma) \tag{27b}$$

$$v_{KS}(\boldsymbol{r}, \sigma) = v_N(\boldsymbol{r}) + v_H(\boldsymbol{r}) + v_{XC}(\boldsymbol{r}, \sigma) \tag{27c}$$

where $\hat{F}$ is the KS operator consisting of a kinetic term and the effective potential $v_{KS}(\boldsymbol{r},\sigma)$. Potential v_{KS} in turn contains a term v_N for the nucleus–electron attraction, v_H for the classical electron–electron repulsion, and v_{XC} for the description of exchange (X) and correlation (C) effects. In distinction to the potential term occurring in many-body Schrödinger theory, potential v_{KS} depends through v_H and v_{XC} on the electron density and thus needs to be determined self-consistently together with the KS orbitals ψ_p. The form of v_H for a given electron density follows from electrostatics, whereas the exact form of v_{XC} is not known, and approximate functionals for the XC energy E_{XC} and the corresponding v_{XC} have to be used in practical DFT computation schemes. Different types of approximate functionals are used for DFT calculations.[81–85] While pure XC functionals express E_{XC} exclusively through the one-particle density,[81–84] in hybrid DFT functionals a part of the X energy is expressed exactly by the KS orbitals.[85] Generally, hybrid functionals allow more accurate SSCC calculations, at the cost of higher computational expenses,[58] because they largely suppress the self-interaction error of KS-DFT.[86–89]

Starting from the coupled perturbed DFT (CP-DFT) approach, an expression for the calculation of SSCC in the framework of KS-DFT was derived for the first time in ref. 58. The final expression for the four Ramsey terms takes the form:

$$K_{AB}^{\mathrm{DSO}} = \sum_{i}^{\mathrm{occ}} \langle \psi_i | \hat{K}_{AB}^{\mathrm{DSO}} | \psi_i \rangle \tag{28a}$$

$$K_{AB}^{\mathrm{PSO}} = -\frac{2}{3} \sum_{i}^{\mathrm{occ}} \sum_{a}^{\mathrm{unocc}} (\varepsilon_a - \varepsilon_i)^{-1} \langle \psi_i | \hat{\boldsymbol{B}}_A^{\mathrm{PSO}} | \psi_i \rangle \langle \psi_i | \hat{\boldsymbol{B}}_B^{\mathrm{PSO}} + \tilde{\boldsymbol{F}}_B^{\mathrm{PSO}} | \psi_i \rangle \tag{28b}$$

$$K_{AB}^{\mathrm{FC}} = -\frac{2}{3} \sum_{i}^{\mathrm{occ}} \sum_{a}^{\mathrm{unocc}} (\varepsilon_a - \varepsilon_i)^{-1} \langle \psi_i | \hat{\boldsymbol{B}}_A^{\mathrm{FC}} | \psi_i \rangle \langle \psi_i | \hat{\boldsymbol{B}}_B^{\mathrm{FC}} + \tilde{\boldsymbol{F}}_B^{\mathrm{FC}} | \psi_i \rangle \tag{28c}$$

$$K_{AB}^{\mathrm{SD}} = -\frac{2}{3} \sum_{i}^{\mathrm{occ}} \sum_{a}^{\mathrm{unocc}} (\varepsilon_a - \varepsilon_i)^{-1} \langle \psi_i | \hat{\boldsymbol{B}}_A^{\mathrm{SD}} | \psi_i \rangle \cdot \langle \psi_i | \hat{\boldsymbol{B}}_B^{\mathrm{SD}} + \tilde{\boldsymbol{F}}_B^{\mathrm{SD}} | \psi_i \rangle \tag{28d}$$

The final expressions resemble those for the many-body formalism (see eqn (25)). However, there are some important differences:

(i) Expectation values are formed with KS orbitals rather than the many-body wave function.

(ii) Energy denominators are formed with the KS orbital energies rather than the energies of the many-electron eigenstates. (iii) The KS potential appearing in the KS equations depends on the electron density self-consistently, which leads to the fact that in addition to the explicitly given operators $\hat{\boldsymbol{B}}_A^X$ (X = PSO, FC, SD), one has to consider the operator $\tilde{\boldsymbol{F}}_B^X$ that reflects the feedback of the perturbed KS orbitals on the *XC* potential. The operator $\tilde{\boldsymbol{F}}_B^X$ is connected with the first-order spin orbitals $\vec{\psi}_i^{(X),B}$ (for a perturbation of the type X at nucleus B, the Cartesian components of $\vec{\psi}_i^{(X),B}$ correspond to the Cartesian components of the perturbation) by the equations

$$\tilde{\boldsymbol{F}}_B^X = \sum_{i}^{\mathrm{occ}} \int \mathrm{d}^3 r \frac{\delta F}{\delta \psi_i(\boldsymbol{r})} \vec{\psi}_i^{(B),X}(\boldsymbol{r}), \tag{29a}$$

$$|\vec{\psi}_i^{(B),X}\rangle = -\sum_{a}^{\mathrm{unocc}} \frac{\left\langle \psi_a^{(0)} | \hat{\boldsymbol{B}}_B^X + \tilde{\boldsymbol{F}}_B^X | \psi_k^{(0)} \right\rangle}{\varepsilon_a - \varepsilon_i} |\psi_a^{(0)}\rangle \tag{29b}$$

where $\delta F/\delta \psi_i(\boldsymbol{r})$ is the functional derivative of $\hat{F}$ with respect to the KS orbital ψ_i. Eqns (29a) and (b) need to be solved self-consistently for $\tilde{\boldsymbol{F}}_B^{\mathrm{FC}}$ and the perturbed orbitals $\vec{\psi}_i^{(B),X}$. This is by far the most expensive part in solving the CP-DFT equations. It should be noted that $\tilde{\boldsymbol{F}}_B^{\mathrm{PSO}}$ will vanish if a pure DFT functional is used, *i.e.* for pure DFT functionals, K_B^{PSO} does not need to be determined iteratively.

Neglecting $\tilde{\boldsymbol{F}}_B$ in eqn (29a) and (29b) leads to sum-over-states density functional perturbation theory (SOS-DFPT), which can be performed non-iteratively on the basis of a conventional KS-DFT calculation. SOS-DFPT amounts to neglecting the impact of electron–electron interaction on the response of the perturbed system, which is not justified *a priori*. In refined versions of SOS-DFPT, the neglect of $\tilde{\boldsymbol{F}}_B$ is partly compensated by corrections to the energy denominators in eqn (29a) and (29b). Calculations by Bouř *et al.*[90] showed that an SOS-DFTP approach, even with correction terms in the energy denominators, does not allow a quantitative prediction of SSCCs.

As has been shown,[91] conventional DFT is not strictly valid in the presence of a magnetic field. Rather, the formalism has to be extended to current-DFT, where the *XC* potential depends not only on the one-electron density but also on the one-electron current density. However, to date no approximate expressions for such a current-dependent *XC* potential are available that are suitable for routine applications. Therefore, the current dependence of the *XC* functional is usually neglected in present DFT calculations of magnetic properties.[92]

3. Empirical relationships utilizing SSCCs as descriptors for bonding and the electronic structure of a molecule

Early experimental and theoretical work in NMR spectroscopy emphasized that SSCCs are ideally suited to determine configuration and conformation of molecules. The first major breakthrough in this respect was Karplus' observation that vicinal SSCC $J(A,D)$ in a fragment A–B–C–D depend on the dihedral angle $\tau(ABCD)$ *via* a trigonometric relationship.[33–35] Karplus' discovery led to a flood of experimentally or computationally derived Karplus equations varying atoms A, B, C, D through larger parts of the periodic table, especially however with regard to those elements typically found in organic compounds.[30–32,93] Work of more than four decades has led from Karplus equations to Karplus surfaces where beside a single dihedral angle also adjacent bond angles, a second dihedral angle, the orientation of substituent bonds or the electronegativity of the latter was included.[93–95] The term *generalized Karplus equation* was used in this connection and applied to the description of puckered and pseudorotating rings. Cremer and co-workers[96–98] demonstrated that in the latter case, the vicinal SSCC is best expanded as a function of the Cremer-Pople ring puckering coordinates[99–101] in form of a generalized Karplus surface, which reflects preferred ring conformations and pseudorotational modes.

SSCCs also depend on other geometric parameters such as bond distances or bond angles. In many studies measured or calculated SSCCs (one-bond, geminal, vicinal, long range) were related to bond or internuclear distances (through-bond or through-space distances),[28–32,102–104] bond or pyramidalization angles, lone pair or substituent orientations, the distance to neighboring charges exerting an electric field effect, or other geometric parameters. (For summaries, see ref. 28–32).

At an early stage, Muller and Pritchard[105,106] demonstrated that the FC part of ^1J(C,H) could be related to the degree of sp-hybridization at the C atom. Since the FC term dominates the SSCC of hydrocarbons in most cases this discovery was understood in an enthusiastic way as a direct experimental possibility of describing bonding: once the degree of sp-hybridization is known for the C atoms of a molecule, the overlap between the hybrid orbitals is found by considering measured bond lengths and in this way a reasonable estimate

of the bond strength can be given using the maximum overlap method. In this spirit numerous relationships were developed that related one-bond SSCCs to the square of the valence s-character (AH bonds),[7,28,29,107] the product of the s-characters of coupling nuclei A and B (AB bonds)[7,28,29,108] and/or the overlap $S(A,B)$.[109,110] Some of these relationships are still used today although they all have in common that any application of these relationships beyond a limited set of bond situations (*e.g.* including besides single bond also multiple bonds) leads to relatively large deviations from the original functional dependencies between SSCC and s-character.[7,30–32]

Triggered by investigations showing a relationship between s-character and the magnitude of the SSCC in hydrocarbons, one soon established also relationships with the bond order,[104,111–115] especially the π-bond order in conjugated systems, delocalization parameters, NBO occupation numbers[115] or charge parameters.[116] An astonishingly accurate relationship between ^1K(X,H) and the atomic number Z of X was discovered[117] (originally already discussed by Jameson and Gutowsky relating Z to the s-electron density at the nucleus[107]) where however for X of fourth and higher periods reliable experimental data were missing.

In summary, the multitude of empirical relationships available gives the impression that SSCCs are perfectly suited to describe the quantum mechanical implications of chemical bonding and the electronic structure of a molecule. This however is rarely the case in state-of-the-art studies on SSCCs. Instead, the relationships discussed are mostly used to estimate SSCCs of new chemical compounds in an empirical way. This is a reflection of the fact that none of the relationships relating SSCCs to some molecular parameters in an empirical way is based on a quantum mechanical analysis of the spin–spin coupling mechanism considering all four Ramsey contributions. Mostly, it is assumed that the FC part dominates the magnitude of the SSCC and FC coupling is related in some way to the s-electron density at the nucleus. Insofar it is justified to say that a systematic quantum mechanical analysis of all Ramsey terms of SSCCs as descriptors of the electronic structure of molecules has not been carried out at all. J-**OC**-PSP presents for the first time such a complete and systematic analysis of SSCCs by following strictly the quantum mechanical description of the spin–spin coupling mechanism rather than referring to empirically derived relationships with limited applicability.

4. Analysis of the spin–spin coupling mechanism

In the previous sections, we have given an overview over the physics of NMR spin–spin coupling, the DFT calculation of SSCCs, and those attempts that have been made to analyze the spin–spin coupling mechanism. Before we present the J-**OC**-PSP method, it is useful to determine those requirements that an analysis method must fulfill to provide useful results of general and not method-dependent value.

4.1 Basic requirements for an analysis of the spin–spin coupling mechanism

A theoretical analysis of NMR SSCCs must fulfill a set of 9 requirements (a)–(i):

(a) Reciprocity requirement: any useful analysis must lead to a description of the spin–spin coupling mechanism that is independent of the choice of perturbing and responding nucleus.

(b) Requirement of unconstrained applicability: a useful analysis must be applicable to all four Ramsey terms of the isotropic SSCC or the nondiagonal coupling terms of the SSCC tensor. Also it must be applicable to any type of spin–spin coupling (one-bond, two-bond or long range coupling, through-bond or through-space coupling, across H-bond coupling, *etc.*) between any possible combination of nuclei.

(c) Correct reflection of the physics of spin–spin coupling: (I) Any analysis must be able to resolve and analyze steps (i), (ii), and (iii) of the spin–spin coupling mechanism:

(i) The perturbing nucleus B induces changes in the electron system.

(ii) These changes propagate through the electron system.

(iii) The changes in the electron system generate an extra magnetic field and can thus be sensed by the responding nucleus A.

(II) Because of the reciprocity of spin–spin coupling, the analysis of (i) and (iii) should be largely analogous.

(III) Furthermore, Fermi coupling between nuclear and electronic spin, electron–electron exchange interactions, and Pauli spin-pairing between electrons must be correctly reflected by the mechanistic analysis.

(d) Requirement of a parallel-processing analysis: a corollary of (c) is the need that the analysis method in question is carried out parallel to the calculation of the SSCC (parallel-processing method) rather than afterward (post-processing method). Only in this way is it possible to follow the stepwise spin–spin coupling process.

(e) Insight beyond the quantum mechanical SSCC formulae: Any analysis must reflect the anisotropy of DSO, PSO, and SD term by spatial decomposition in Cartesian components, provide a distinction between one-electron and electron–electron-interaction contributions, and must distinguish between different coupling paths.

(f) Use of reasonable analysis quantities: preferably, any analysis of the spin–spin coupling mechanism should be based on quantities that are generally used in quantum mechanics as, *e.g.*, orbitals, electron density distributions (especially spin density distributions), and energy density distributions. In view of the description of spin–spin coupling utilizing perturbation theory, the roles of perturbed orbitals (first order orbitals) and perturbed electron densities (first order densities) have to become clear.

(g) Usefulness of results: any useful analysis of the spin–spin coupling mechanism must lead to results that describe the mechanism in a compact manner and can be directly related to accepted quantum mechanical descriptions of chemical bonding and electronic structure.

(h) Additivity requirement: any partitioning of the SSCC must lead to contributions that sum up to the four Ramsey terms and the total SSCC.

(i) Feasibility requirement: any analysis of the spin–spin coupling mechanism must still be feasible in terms of computational requirements and computational cost.

The way of calculating SSCC *via* the use of orbitals (section 2) suggests that orbitals are also employed when analyzing the spin–spin coupling mechanism. Without limiting any SSCC analysis to the use of a special type of orbitals, a number of additional requirements can be formulated for an orbital-based analysis method:[68]

(1) The analysis must be capable of distinguishing between one-, two- and *m*-orbital contributions where each of these terms should be connected with a well-defined physical effect.

(2) The orbital contributions must fulfill the criterion of nuclear independence, *i.e*. the same orbital contributions must be obtained irrespective of the choice of perturbing and responding nucleus, *i.e*. the direction of the spin–spin coupling mechanism (see requirement (a) above).

(3) The orbital contributions should be based on the analysis of zeroth- and first-order orbitals rather than just the total perturbed orbitals. In this connection, any ambiguity in choosing the first-order orbitals must be treated in a well-defined way.

(4) It must be possible to distinguish between active and passive orbital contributions to the spin–spin coupling mechanism. Active orbitals are exclusively involved in the one- and two-orbital contribution, whereas passive orbitals lead to three- and *m*-orbital contributions ($m > 3$).

(5) The method in question should not be tied to a particular type of molecular orbitals.

(6) The individual orbital contributions obtained in the analysis should add up to the total SSCC or its Ramsey terms (see requirement (h) above).

(7) For the anisotropic Ramsey terms (PSO, DSO and SD), it must be possible to perform the analysis for either the isotropic average of the terms or their Cartesian components (see requirement (e) above).

(8) A pictorial description of the orbital terms in a way that the spin–spin coupling mechanism can be stepwise followed is necessary.

Previous analysis methods were not able to meet either requirements (a) to (i) nor (1) to (8). In section 4.2, we will show that J-**OC**-PSP is able to comply with all requirements.

4.2 The J-OC-PSP method

A decomposition of the total spin–spin coupling into contributions from individual mechanisms can be carried out according to different decomposition criteria. The J-**OC**-PSP analysis method utilizes five decomposition criteria, denoted (I)–(V) in the following, where each of these criteria spans one dimension in the space of the analysis. Fig. 1 shows the three most important of these criteria in form of an incomplete cubic space:

(I) Ramsey decomposition. The four Ramsey terms described in sections 2.5 and 2.6 provide one way to decompose the total spin–spin coupling into individual contributions. (See horizontal axis in Fig. 1.)

(II) Orbital decomposition. This is characterized according to the number and kind of orbitals involved in the spin-information transport through the electron system (step (ii) of the 3-step mechanism; vertical axis in Fig. 1). In the simplest case, the perturbing nucleus (B) affects orbital k, which directly transfers the spin information to the responding nucleus (A):

$$(B) \rightarrow k \rightarrow (A) \qquad (30a)$$

If k is an orbital in the bond path between (A) and (B), the contribution (30a) will be denoted as bond contribution (see Fig. 2a and b), otherwise, *i.e*. if k is external to the bond path (A) – (B), an external bond contribution (see Fig. 2c and d). However, processes involving more than one orbital play an important role in spin–spin coupling.[66,68] A change in one orbital can cause changes in other orbitals in the way that spin information is transferred along paths involving an arbitrary

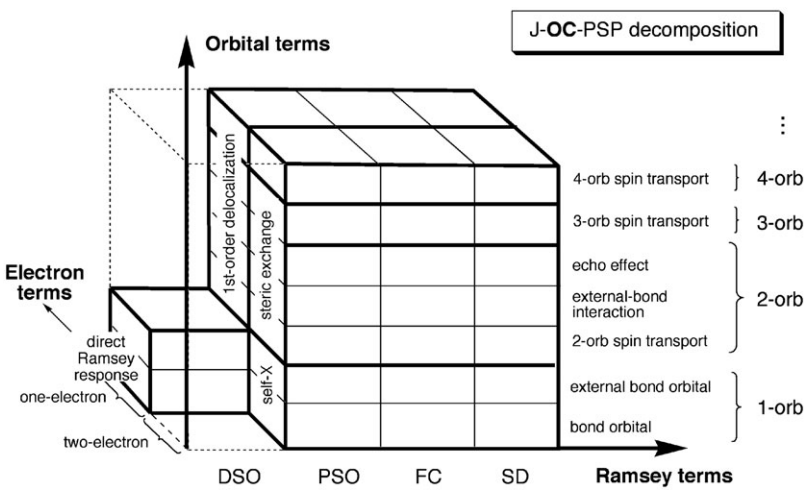

Fig. 1 J-**OC**-PSP decomposition criteria I (Ramsey terms), II (orbital terms), and III (electron terms) of the SSCC shown in 3-D space. Abbreviation orb denotes the term orbital.

number of orbitals:

$$(B) \rightarrow k \rightarrow l \rightarrow (A) \qquad (30b)$$

$$(B) \rightarrow k \rightarrow m \rightarrow l \rightarrow (A) \qquad (30c)$$

$$(B) \rightarrow k \rightarrow m \rightarrow n \rightarrow l \rightarrow (A) \qquad (30d)$$

$$(B) \rightarrow k \rightarrow m \rightarrow k \rightarrow (A) \qquad (30e)$$

These orbital paths describe a variety of coupling processes:

(1) In (30b), the perturbing nucleus affects orbital k, which in turn affects orbital l; nucleus (A) senses the change in orbital l. If k and l are in the bond path between (A) and (B) (see Fig. 2e and f), this process will be denoted as *direct spin transport*; if k or l are external to the bond path (see Fig. 2g), as *external bond interaction*.

(2) In (30c), the spin information is transferred from k to l by mediation of a third orbital m (Fig. 2h); in (30d), the path is extended by another orbital n (Fig. 2i). Processes of this type will be called *3-orbital, 4-orbital, etc. spin transport*.

It is noteworthy that orbitals k, l as opposed to orbitals m, n play different roles in the transmission of spin information: whereas k, l interact directly with one (or both) of the coupling nuclei, m, n participate in the spin–spin coupling solely by interactions with other orbitals, *i.e.*, they do not "see" any of the coupling nuclei. We call orbital contributions that involve direct interaction with one or both coupling nuclei *active contributions*, orbital contributions involving no such direct interactions are called *passive contributions*. In the same way, we speak of *active* and *passive orbitals*.

(3) An orbital path may also contain one and the same orbital several times. In (30e), (B) affects orbital k, which in turn affects orbital m. The change in m is then fed back into orbital k, which passes the spin information to nucleus (A). Orbital m generates an "echo" in orbital k and therefore this kind of process is called *echo effect* (Fig. 2k).

The total spin–spin coupling is the sum of the contributions from all orbital paths. An orbital that makes an active contribution in one path may make a passive contribution in another path. Also, an orbital may make both kinds of contributions in one and the same path, as *e.g.* orbital k in the path

$$(B) \rightarrow k \rightarrow l \rightarrow k \rightarrow m \rightarrow k \rightarrow (A) \qquad (30f)$$

Keeping track of all individual orbital paths would make the analysis both time-consuming and produce a large amount of information that would be difficult to comprehend. In particular, one and the same set of orbitals can form a variety of orbital paths, *e.g.*, (30c) as well as (30f) involve k, l and m. Therefore, the J-**OC**-PSP analysis focuses on the role individual orbitals or groups of orbitals (summed up over all possible orbital paths) rather than individual orbital paths play for spin–spin coupling.

The DSO term differs from the FC, SD, and PSO terms as it does not involve any changes in the orbitals. There are no orbital interactions in the DSO mechanism, nor any passive contributions. Consequently, the DSO term consists solely of active one-orbital contributions (see Fig. 1).

The calculation of orbital contributions is the key part of a J-**OC**-PSP analysis. For the purpose of determining the role of a given orbital, one performs a number of calculations for a given SSCC. In these calculations, the orbitals under consideration will be allowed to participate in the spin–spin coupling in different ways:

(a) An *active orbital* is allowed to interact both with the coupling nuclei and the other orbitals. It may thus make active as well as passive contributions to the spin–spin coupling mechanism.

(b) A *passive orbital* is allowed to interact with other orbitals but not with the coupling nuclei. It is thus restricted to passive contributions.

(c) A *frozen orbital* is not allowed to undergo any interactions, *i.e.*, it is "frozen" in the shape it has when the perturbation is absent. Accordingly, a frozen orbital cannot make any contributions to the coupling.

By comparing calculations for one and the same SSCC, one can identify the active and passive contributions the individual orbitals make to the coupling.[62] In principle, one can refine the analysis of orbital contributions by selecting not only occupied but also unoccupied (virtual) orbitals. For instance, instead of freezing an orbital completely one might restrict excitations from those orbitals to selected virtual orbitals. An extension of J-**OC**-PSP in this spirit would be straightforward. However, a number of reasons speak against such an extension: the structure (number, energy, and shape) of the unoccupied orbitals is sensitive to the method (in case of DFT: sensitive to the *XC* functional) and especially the basis set used. Apart from this, the localization of unoccupied orbitals may be problematic, *e.g.*, it may give rise to artificial symmetry breaking. In addition, a decomposition into contributions from individual virtual orbitals will drastically increase the number of J-**OC**-PSP contributions and make the analysis less comprehensible. A more appropriate approach is therefore to plot and analyze the first-order perturbed orbitals, as is demonstrated in sections 4.5 and 4.6.

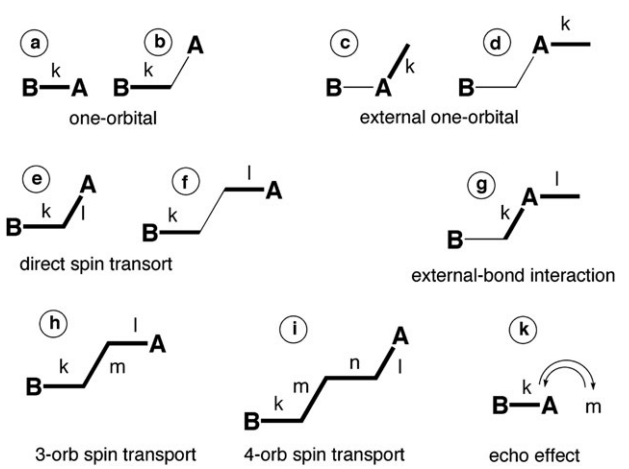

Fig. 2 Schematic representation of different orbital contributions. Bold lines symbolize an involvement of the corresponding bond orbital (orb: orbital). (A) is the responding, (B) the perturbing nucleus.

(III) One- and two-electron contributions. This decomposition criterion is given by the third axis in Fig. 1 and can be explained along the following lines. Each space orbital can be occupied by two electrons with opposite spin. Accordingly, a

one-orbital contribution to a SSCC can comprise two kinds of processes:

(a) The spin information may be conveyed from (B) to (A) by one of the electrons without any involvement of the second one. This kind of transport mechanism will be called *direct Ramsey response*.

(b) The interaction between the electrons in the orbital enhances the response of the orbital to the perturbation, which can be easily explained for the FC term: the magnetic moment of the nucleus attracts the β electron (*Fermi coupling*) and repels the α electron. Consequently, the electrons in the orbital get spin-polarized, and the centroids of charge associated with the two electrons are slightly shifted against each other. This gives rise to an electrostatic repulsion force between the β and the α electron, which tends to increase spin polarization and thus amplifies the response of the orbital to the perturbation from (B). Since Hartree repulsion between the electrons must not be changed by any magnetic perturbation, this effect implies a maximization of the (negative) self-exchange energy for the two electrons. Therefore it is justified to call this effect *self-exchange interaction*.

As regards two- or more-orbital contributions, there are two mechanisms for the spin-information transfer from one orbital to the next:

(c) If orbital l changes its shape by mixing with the virtual orbital a (described by excitation $l \rightarrow a$ and caused by the magnetic perturbation) then the one-particle energy has to be re-optimized in the way that orbital k undergoes a small delocalization $k \rightarrow l$, which has to be accompanied by a partial excitation $k \rightarrow a$ to maintain orthogonality. This effect provides an interaction between perturbed (first order) orbitals k and l which does not involve electron–electron repulsion. This interaction is a consequence of the Pauli principle and related to the well-known orbital delocalization effect of unperturbed orbitals (zeroth order orbitals). Therefore, this effect is called *first order delocalization*.

First-order delocalization effects do not occur when (delocalized) canonical molecular orbitals (CMOs) are used for the description of spin–spin coupling. Although this might be considered as a way of simplifying the analysis, CMOs have the disadvantage of disguising an important source of information about the coupling mechanism. LMOs reveal how spin information is conveyed from orbital to orbital *via* first order delocalization, whereas in a CMO description this effect is hidden in the shape of the orbitals.

(d) If orbital l undergoes a change, then orbital k will re-optimize its shape such that the exchange interaction between the electrons in k and l is maximized, *i.e.* the overlap between equal-spin orbitals is maximized and that between opposite-spin orbitals is minimized. This effect is related to the steric repulsion in chemistry and will therefore be called *steric exchange interaction*.

Given the ambiguity in the choice of the orbitals, neither effects (a) and (c) nor effects (b) and (d) can be separated strictly. Both (a) and (c) describe the spin–spin coupling processes at the one-electron level, whereas (b) and (d) reflect the impact of electron–electron interactions on the spin–spin coupling. Effects (b) and (d) can eventually be related to the minimization of $\alpha \leftrightarrow \beta$ overlap for the electrons in the perturbed molecule.

Similarly as for decomposition criterion III, the DSO term is different from the other three terms in that there are no electron-interaction contributions. As there are no orbital-interaction terms either, only case (a) is relevant for the DSO term (Fig. 1).

The separation of the total SSCC into one- and two-electron contributions can be done as described in ref. 69: all orbital contributions of interest are calculated at the CP-DFT level and at the SOS-DFPT level. The SOS-DFPT calculation will provide the one-electron part (*i.e.*, effect (a) or (c)) for the respective orbital contribution as was explained in section 2.7 whereas the difference between CP-DFT and SOS-DFPT results will yield the two-electron part (*i.e.*, effect (b) or (d)).

(IV) Lewis and non-Lewis contributions. Even in an LMO description, the MOs comprise delocalization tails indicative of, *e.g.*, conjugation effects. These delocalization tails can play a crucial role for the transport of spin information, especially for higher-order SSCC's, because they may establish efficiently contact to other orbitals or to the coupling nuclei. The contribution of these delocalization tails to the SSCC can be quantified by decomposing each occupied orbital into a so-called Lewis part, which reflects the character of the orbital in the Lewis scheme (*i.e.*, bond, lone pair, or core orbital), and a non-Lewis part, reflecting all delocalization effects not described in the Lewis scheme.[68] The J-**OC**-PSP approach is able to cover both the Lewis and the non-Lewis parts of spin–spin coupling.[68] For this purpose, one proceeds as follows:

(a) One starts with a J-**OC**-PSP analysis as described in (II).

(b) One determines the natural bond orbitals (NBOs) of the unperturbed system.[118]

(c) The electron structure of the unperturbed system is then modified such that all Lewis NBOs are doubly occupied whereas all non-Lewis orbitals are kept unoccupied.

(d) The J-**OC**-PSP analysis is redone starting from this modified electron structure.

The results obtained in step (d) can be considered as Lewis contributions, whereas the difference between the results from steps (a) and (d) determines the impact of the non-Lewis contributions, *i.e.* thus providing the delocalization features to spin–spin coupling.

(V) Cartesian components. Even though only the isotropic average of the SSCC tensor can be observed in experiment the decomposition of SSCC into their Cartesian contributions provides additional insight into the coupling mechanism and can be related to the anisotropy of the electron density distribution.[70]

The J-**OC**-PSP method is set up in a way that the individual J-**OC**-PSP contributions are reciprocal as was required in section 4.1: each J-**OC**-PSP contribution can be formulated as a mixed derivative of a properly chosen energy expression with respect to $\vec{\mu}_A$ and $\vec{\mu}_B$, or their Cartesian components. The value of such a mixed derivative does not depend on an interchange of nuclei A and B.

As is shown in Fig. 1 for (I)–(III), one can in principle apply all dimensions (decomposition criteria) of the analysis simultaneously, *i.e.*, decompose the total SSCC into Ramsey terms,

each Ramsey term (except the DSO term) into one-electron and two-electron contributions, each one-electron contribution into direct Ramsey response and first-order delocalization, *etc*. However, there are a number of reasons why such a complete analysis is more the exception than the rule:

(i) The large number of terms resulting, if calculated on a routine basis, is expensive to compute.

(ii) The amount of data makes it difficult to rationalize the results.

(iii) Apart from this, many of the contributions shown in Fig. 1 can be expected to be small, *e.g*., two-electron contributions to the PSO term are small in most cases.

Therefore it is advisable to select for each SSCC problem those decomposition criteria and that level of detail that is of interest for the questions to be answered. Often the investigation is refined for individual terms in an iterative process where one *e.g*. starts with an investigation along (I) and (II) and then considers (III), (IV), or (V) for selected terms. Thus, the J-**OC**-PSP analysis may be seen as a versatile ''tool box'' rather than a rigid algorithm for the investigation.

4.3 Computational considerations

The computational realization of the J-**OC**-PSP method is described in detail in ref. 61–64, 68 and 69. The basic idea is to perform a number of calculations for each SSCC under consideration where in each calculation selected orbitals are either *kept passive*, *i.e*., their interaction with the coupling nuclei is switched off, or *kept frozen*, *i.e*., the orbitals are kept fixed to the shape they have without the magnetic perturbation. The J-**OC**-PSP contributions are then obtained as the difference of the SSCC values for different sets of passive or frozen orbitals.

The idea of the J-**OC**-PSP analysis is initially not tied to a particular method to calculate the SSCC. However, the properties of the algorithm lead to a number of requirements: (i) The calculation method needs to be efficient, as a number of SSCC calculations is required for each pair of coupling nuclei. (ii) The method is based on an orbital picture, with a sharp distinction between occupied and unoccupied orbitals. Thus, the method should provide orbitals in a natural way. (iii) Clearly, to be applicable, the method has to provide reliable values for the SSCC.

The DFT calculation of SSCCs[58] meets these criteria, providing a relatively cheap but still reliable calculation of SSCCs and a representation of the results in terms of zero- and first-order KS orbitals. Therefore, the method has been implemented as an extension of our code for the DFT calculation of SSCCs contained in the COLOGNE 2006 package.[119] COLOGNE 2006 allows to solve the CP-DFT equations in terms of LMOs, *i.e*., the J-**OC**-PSP algorithm could be integrated into the code for SSCC calculations in a natural way.

The J-**OC**-PSP analysis can be performed in any kinds of canonical or non-canonical MOs. To comprehend the coupling mechanism in the best possible way, one should use a set of orbitals that suits the chemist's intuitive understanding of bonding and electronic structure in terms of bonding, lone pair, or core electrons. Therefore, the J-**OC**-PSP analysis is usually performed in terms of LMOs. The proper choice of the LMO's is critical for the relevance of the J-**OC**-PSP results.[61,68] Natural LMOs (NLMOs) have a similar shape as, *e.g*., LMOs obtained from a Boys localization,[120] however they lead, contrary to Boys-localized LMOs, to unreasonable orbital contributions, due to their construction. NLMOs are formed from natural atomic orbitals (NAOs), which implies that the NLMO core orbitals contain tails made up from valence shell orbitals. Analogously, the bond and lone pair NLMOs become contaminated by the core orbitals. This mixing between different types of orbitals in the NLMOs gives rise to artifacts in the J-**OC**-PSP contributions reflected by relatively large core orbital contributions to the spin–spin coupling mechanism, which are mechanistically seen unreasonable. Boys-localized orbitals[120] do not show these artifacts, provided that the localization is performed separately for groups of orbitals (core, σ valence orbitals, π orbitals). Therefore, Boys-localized orbitals are preferentially used for the J-**OC**-PSP analysis.

In the following we will demonstrate the usefulness of the J-**OC**-PSP analysis method for the example of the one bond coupling constant of FH.[70] The experimental gas phase $^1J(^{19}F,^1H)$ value is 529 Hz,[121] which has to be corrected for vibrational contributions to compare it with the calculated value. In recent years, various ways of calculating vibrational corrections for SSCCs have been developed[122–125] and it has been shown that their magnitude can be substantial. In the case of the one-bond FH SSCC calculated vibrational contributions vary between 26 and 37 Hz[126,127] thus corresponding to (equilibrium) J_e constants between 555 and 566 Hz. These values agree reasonably with the 553 Hz obtained in a BLYP(60,40) calculation at R_e(FH) = 0.9169 Å , in which 60% of exact exchange and 40% of Becke exchange[58] have been used together with a large (15s6p3d1f/10s3p1d) [15s4p3d1f/10s3p1d] basis set to describe FC and PSO term reasonably accurately.[70] According to this calculation, the FC term contributes 355 Hz, the PSO term 204 Hz whereas SD (−6 Hz) and DSO terms (0.2 Hz) are small.[70] The SSCC is large because the magnetogyric ratio of both the proton (26.7522×10^7 rad T^{-1} s^1) and ^{19}F (25.1815)[76] are rather large. Normally, one analyzes the reduced SSCC K to exclude the influence of the magnetogyric ratios and to obtain comparable quantities. In the present case, we consider SSCC J because we want to consider just the usefulness of J-**OC**-PSP.

4.4 The spin-polarization terms

The first mechanism for the transfer of spin information between perturbing (H) and responding nucleus (F) is provided by spin-polarization of the electron density distribution. As pointed out in section 2.6, the electrons can interact with the magnetic field of the nucleus in two ways (see Fig. 3).

(a) The internal uniform magnetic field of the nucleus can only be experienced by those electrons which have a finite probability of being located at the *contact surface* of the nucleus, *i.e*. only the s-electrons can ''see'' the internal magnetic field of the nucleus (lower part of Fig. 3). Accordingly, s-orbitals are in this case active orbitals, which does not exclude that s-density, once spin polarized, passes on spin polarization to other electrons that do have a zero-probability of being

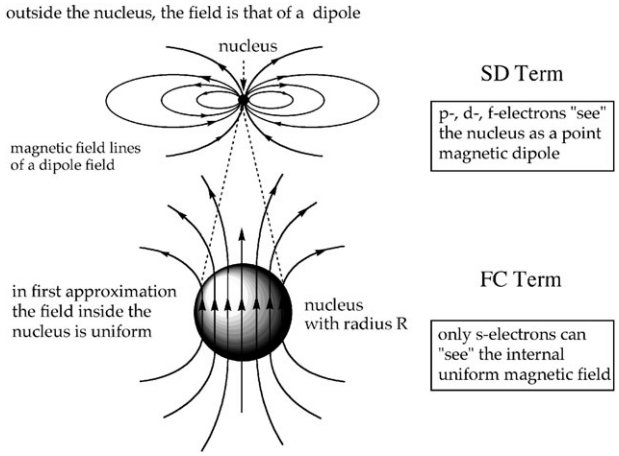

Fig. 3 Magnetic field of a finite nucleus with radius *R*. In the lower part of the drawing, the nucleus with radius *R* is enlarged to see the internal uniform magnetic field.

located at the contact surface (p-, d-, f-electrons). Active and passive contributions together establish the FC coupling mechanism.

(b) The FC-passive electrons "see" the external dipole field of the nucleus and therefore they become spin polarized (upper part of Fig. 3). When they pass this spin polarization directly or indirectly to the responding nucleus, the SD term results.

Although both FC and SD coupling mechanisms follow the three-step transfer mechanism described above, they differ in one fundamental aspect, which is reflected by the form of the FC and SD operators discussed in section 2.6. The former is an isotropic operator (because its kernel is the Dirac delta operator $\delta(\boldsymbol{r}_{iA})$, see section 2.6) that leads just to one contribution (per orbital) whereas the latter is an anisotropic operator that has to be isotropically averaged. First, we will consider the FC coupling mechanism.

4.4.1 The Fermi contact (FC) coupling mechanism. A typical explanation of the ^1J(F,H) value would use a *Dirac vector model* of spin–spin coupling to predict the dominant mechanism and the sign of the SSCC (see Fig. 4). Assuming α spin for the perturbing nucleus H, the Fermi hyperfine interaction between nucleus and electron should lead to a preference of β spin close to H. The other electron in the bond must have α spin (to comply with the Pauli principle and to maintain spin-neutrality for the bond orbital) and because of electron correlation it should be close to the *F* nucleus, which then as a result of another Fermi interaction prefers β spin. Accordingly, the spins of the coupling nuclei have the favorable α–β configuration thus leading to a positive SSCC. Although this kind of explanation is used often, it is flawed in several ways.

(1) The Dirac vector model describes only the coupling mechanism caused by the FC term. The assumption that the FC term dominates the coupling mechanism is valid only for special situations, however does not hold in general. In the case of the one-bond coupling in FH the PSO coupling mechanism is equally important.

(2) An explanation of spin–spin coupling based on the Dirac vector model as shown in Fig. 4a could be misunderstood in

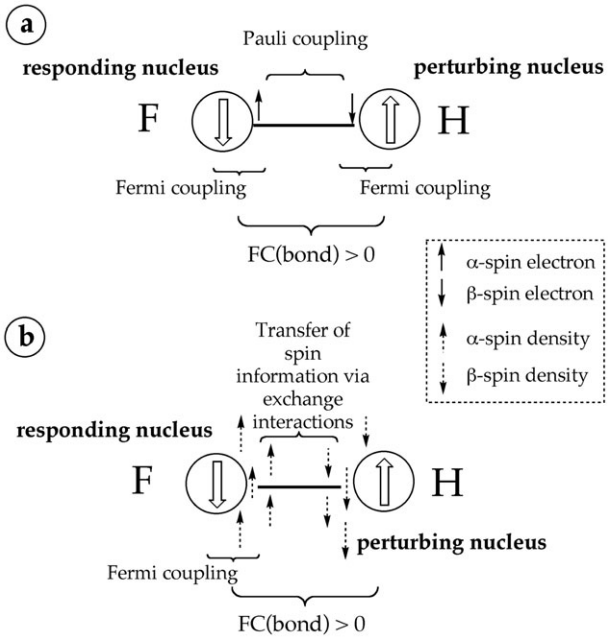

Fig. 4 Dirac vector model of spin–spin coupling (a) in the form normally presented in the literature, (b) in a revised form, which explains the driving force of the FC coupling mechanism. The nuclear spin is indicated by large up (α) and down (β) arrows surrounded by a circle symbolizing the finite size of the nucleus.

the way that the spin transfer mechanism is tuned to Pauli pairing and electron correlation rather than exchange effects. It is correct that β-spin density at the perturbing nucleus H causes more β-spin density withdrawn from the region of F to increase and optimize exchange interactions in the region of the proton. This leads to a dominance of α spin in the region of the F nucleus with the described consequences for Fermi hyperfine coupling at this nucleus. Hence, the maximization of stabilizing exchange interactions, rather than dynamic electron correlation, is the basic spin transfer mechanism indicated by the Dirac vector model. This is more clearly shown in Fig. 3b.

(3) The information provided by the Dirac vector model is valid exclusively for the contact region and not for any other region in the valence shell or bond region. The sign of spin polarization can change several times according to the number and the positions of the nodal surfaces of zeroth- and first-order LMOs in the molecule, which has nothing do with electron correlation or the Pauli principle. The latter is active also without any magnetic perturbation.

(4) One has also to consider that the Dirac vector model refers only to the contribution of the bond orbital, which is just one of several contributions. In the case of FH, the lone-pair contributions may be equally important and their sign cannot be determined with the standard Dirac vector model.

The Dirac vector model can be used to predict the sign of the FC term in the case of two-, three- and *n*-bond spin–spin coupling for acyclic unsubstituted hydrocarbons because for these molecules the bond orbital contributions to the FC coupling mechanism are dominant. Between perturbing and responding nuclei there are one or more nuclei along the

coupling path. One has to consider for these nuclei and the surrounding electron shells the exchange interactions at an atom as described by the intra-atomic Hund rule, which predicts that all valence electrons at an atom involved in bonding possess the same spin. By doing so, the Dirac vector model predicts that the geminal H,H FC coupling term in methane should have a negative sign, the vicinal H,H FC coupling term in ethane a positive sign, *etc.*[15].

After having clarified the contents and the limitations of the Dirac vector model, it is appropriate to describe the FC coupling mechanism in more detail by considering the electron structure of the FH molecule in terms of bond, lone pair, and core LMOs. The bond LMO makes indeed a large positive contribution to the FC term (2055 Hz, Table 1[70]), which is almost six times as large as the FC term itself. To analyze this contribution further, we introduce the FC spin polarization density distribution as a first order density distribution describing the FC coupling mechanism:[61]

$$\begin{aligned} m^{(B),\mathrm{FC}}(\boldsymbol{r}) &= 2\sum_{k}^{\mathrm{occ}}\sum_{\sigma}\psi_{k\sigma}^{(0)}(\boldsymbol{r})\psi_{k\sigma}^{(B),\mathrm{FC}}(\boldsymbol{r}) \\ &= 4\sum_{k}^{\mathrm{occ}}\phi_{k}^{(0)}(\boldsymbol{r})\phi_{k}^{(B),\mathrm{FC}}(\boldsymbol{r}) \end{aligned} \tag{31}$$

where the FC term is given by

$$K_{AB}^{\mathrm{FC}} = \frac{8}{3}\pi\alpha^2\, m^{(B),\mathrm{FC}}(\boldsymbol{R}_A), \tag{32}$$

i.e., the FC term is proportional to the FC spin polarization density at the position of the responding nucleus (A) and the FC spin polarization density is obtained from summing over products of zeroth and first order orbitals. One can split $m^{(B),\mathrm{FC}}$ into one- and two-orbital contributions in the same way as the FC term itself:[61]

$$K_{AB,k}^{\mathrm{FC}} = \frac{8}{3}\pi\alpha^2\, m_{k}^{(B),\mathrm{FC}}(\boldsymbol{R}_A) \tag{33a}$$

$$K_{AB,kl}^{\mathrm{FC}} = \frac{8}{3}\pi\alpha^2\, m_{kl}^{(B),\mathrm{FC}}(\boldsymbol{R}_A) \quad (l \neq k) \tag{33b}$$

where

$$m_{k}^{(B),\mathrm{FC}}(\boldsymbol{r}) = 2\sum_{\sigma}^{\mathrm{occ}}\sum_{a\sigma'}^{\mathrm{virt}}\frac{\left\langle\psi_{a\sigma'}^{(0)}\middle|\boldsymbol{B}_{z}^{(B),\mathrm{FC}} + \tilde{F}_{k,z}^{(B),\mathrm{FC}}\middle|\psi_{k\sigma}^{(0)}\right\rangle}{\varepsilon_k - \varepsilon_a}\psi_{a\sigma'}^{(0)}(\boldsymbol{r})\psi_{k\sigma}^{(0)}(\boldsymbol{r}) \tag{34a}$$

$$m_{kl}^{(B),\mathrm{FC}}(\boldsymbol{r}) = 2\sum_{\sigma}^{\mathrm{occ}}\sum_{a\sigma'}^{\mathrm{virt}}\frac{\left\langle\psi_{a\sigma'}^{(0)}\middle|\tilde{F}_{l,z}^{(B),\mathrm{FC}}\middle|\psi_{k\sigma}^{(0)}\right\rangle}{\varepsilon_k - \varepsilon_a}\psi_{a\sigma'}^{(0)}(\boldsymbol{r})\psi_{k\sigma}^{(0)}(\boldsymbol{r}). \tag{34b}$$

In Fig. 5, the generation of the FC spin polarization density distribution of the FH bond orbital *via* multiplication of the zeroth order bond orbital with the corresponding first order orbital according to eqn (34a) is shown. The sign of the FC coupling term is determined by the signature of the FC spin polarization density at the position of perturbing nucleus (H: negative = β-FC spin polarization density; dashed contour lines; Fig. 5) and responding nucleus (F: positive = α-FC spin polarization density; solid contour lines) and is in line with the prediction made with the help of the Dirac vector model (Fig. 4).[61]

Fig. 5 reveals that the signs of the FC spin polarization density at the coupling nuclei can be anticipated by just

Table 1 FC orbital contributions to the one-bond coupling constants ^1J(FH) in FH[a]

Orbital	Term	FC	SD	PSO	DSO	Total
One-orbital terms						
Bond	Direct Ramsey response	847	−16	−44	−13	774
	Self-exchange interaction	1208	−18	−10	—	1181
	Sum	2055	−34	−54	−13	1955
Lone pair σ	Direct Ramsey response	−393	−2	40	4	−352
	Self-exchange interaction	−183	−1	7	—	−178
	Sum	−576	−3	47	4	−530
Lone pair π	Direct Ramsey response	0	23	124	10	157
	Self-exchange interaction	0	21	78	—	99
	Sum	0	44	202	10	256
Two-orbital terms						
lp σ ↔ *c* external	Steric exchange interaction	−54				−54
bd ↔ lp σ echo	1st order delocalization	56	−1			55
	Steric exchange interaction	69	−2			67
	Sum	125	−3			123
bd ↔ lp σ external	1st order delocalization	−319	−4			−323
	Steric exchange interaction	−763	−9			−772
	Sum	−1082	−13			−1095
Three-orbital terms						
c ↔ bd ↔ lp σ	Steric exchange interaction	−132				−132
σ ↔ π	Steric exchange interaction	30				30
Ramsey terms	Direct Ramsey + 1st order delocalization	191		120	0.2	311
(All orbitals)	Self-exchange + steric exchange	164	−6	84	—	242
	Sum	355	−6	204	0.2	553

[a] All values are given in Hz for the isotopes ^{19}F and ^{1}H. LMO contributions are denoted as c (core), bd (bond), lp (lone pair). For the two-orbital contributions the double-headed arrow indicates that both the contribution $B \rightarrow k \rightarrow l \rightarrow A$ and the contribution $B \rightarrow l \rightarrow k \rightarrow A$ is included.

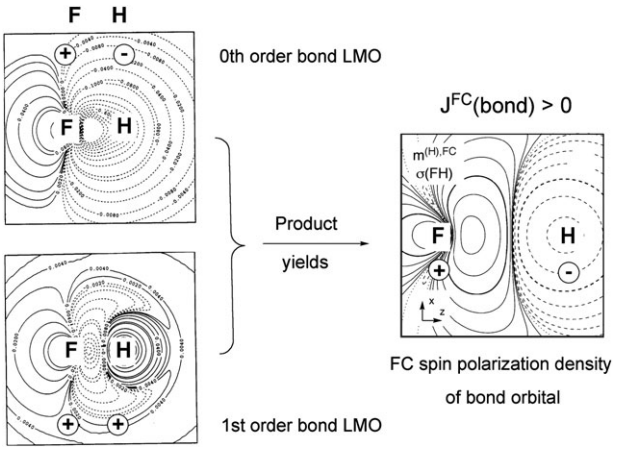

Fig. 5 FC spin polarization density distribution of the FH bond orbital (right side) generated by multiplying the zeroth order bond orbital (upper left) with the corresponding first order orbital (lower left) all given in form of contour line diagrams. Solid contour lines of the FC spin polarization density distribution indicate α, dashed contour lines β FC spin polarization density. For the LMOs, solid (dashed) contour lines denote positive (negative) amplitudes. The signature of LMOs and FC spin polarization density at the coupling nuclei is indicated.

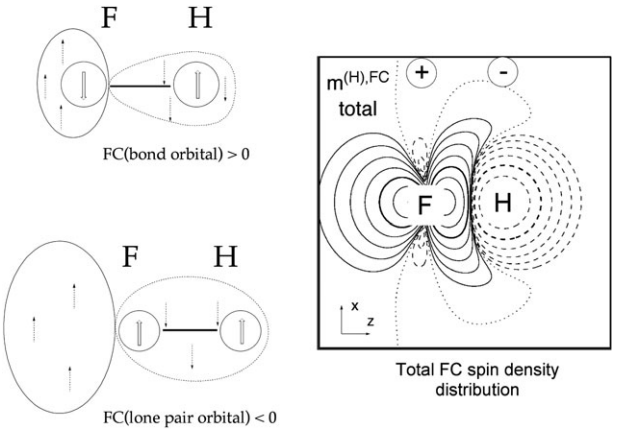

Fig. 6 Total FC spin polarization density distribution of the FH coupling constant given in form of a contour line diagram. Solid contour lines of the FC spin polarization density distribution indicate α, dashed contour lines β FC spin polarization density. The signature of the FC spin polarization density at the coupling nuclei is indicated. The major contributions to the total FC spin polarization density result from the bond orbital and the σ lone pair orbital. The signs of these contributions are given by the extended Dirac vector diagrams on the left side of the drawing (see text).

considering the bonding LMO. For any XH bond of molecules XH_n the bonding LMO has the same signature ratio (+ −) determined by the nodal structure where the number of nodal surfaces increases for X being an element of successively higher periods in the periodic table without changing the signature ratio. In the same way, the signature ratio of the corresponding first order bond LMO (+ + or − −) can be anticipated because this LMO is characterized by the mixing of the zeroth order σ(XH) LMO with a dominant σ*(XH) contribution, which adds one additional nodal surface to the existing nodal structure and, accordingly, leads at one of the nuclei to one sign switch. When forming the FC spin polarization density by multiplication of zeroth order and first order LMO the signature ratio of the former is preserved thus yielding a positive bond orbital contribution to the FC term as discussed above. In these considerations, the phase factor of the zeroth order LMO can be taken freely where, however, the role of perturbing and responding nucleus must be adjusted.

In the same way as the bond orbital contribution can be analyzed it is also possible to analyze and anticipate the sign of all other FC orbital contributions where that of the σ lone pair orbital is the most important one. For zeroth order and first order σ lone pair orbitals there exist again fixed signature ratios at the coupling nuclei (− − or + +) determined by the nodal structures of these LMOs. Again, the first order LMO is characterized by the mixing in of the σ*(XH) LMO which now leads to the adding of two additional nodal surfaces between the coupling nuclei in the way that there is a synchronous change of the signatures at the coupling nuclei in the first order LMO. Again, the signature of the FC orbital contribution is fixed by the signature ratio of the zeroth order orbital at the coupling nuclei. This is used in Fig. 6 to explain why the FC lone pair contribution must be negative utilizing extended Dirac vector diagrams, which show also the zeroth order orbital in question.[61,70]

The distribution of spin in an LMO is given by its nodal structure. The lobe surrounding perturbing nucleus is the region of β electron spin, the adjacent lobe of the LMO separated by a nodal surface the region of α electron spin. If there is just one nodal surface, as in the case of FH, the FC spin polarization density at the responding nucleus will be determined by its position with regard to the nodal surface. If it is in the adjacent lobe, it will be α and the FC contribution is positive (Fig. 6, bond orbital; upper left); if it is in the same lobe, it will be β and the FC contribution is negative (Fig. 6, σ lone pair orbital; lower left). These considerations and the extended Dirac vector diagrams shown in Fig. 6 are valid for any one-bond XH coupling contribution to the FC term as we have shown previously.[61,70]

In Table 1, the one-orbital FC contributions are further analyzed by splitting them in direct Ramsey response and self-exchange interaction part. For the bond LMO, the direct Ramsey response is smaller (847 Hz, Table 1) than the self-exchange part (1208 Hz). This can be explained by considering that the large electronegativity of F leads to a very polar and tight bond orbital difficult to distort. Accordingly, the space confinement leads to a large self-exchange value. The σ lone pair orbital is more diffuse, easier to distort and less confined. Hence, the direct Ramsey response (−393 Hz) becomes absolutely larger than the self-exchange part (−183 Hz). The total contribution of the lone pair orbital (−576 Hz) is smaller than that of the bond LMO (2055 Hz) because of the lower density at H (positioned far out in the diffuse back lobe of the σ lone pair orbital) thus leading to a lower FC spin polarization density at this nucleus.

Since both bond and lone pair LMO are confined in the region of F, a strong steric exchange interaction (−763 Hz,

Table 1) between these orbitals results. One can show using the sign pattern discussed before[61,70] that this must be negative where the steric exchange contribution is absolutely larger than the first order delocalization (−319 Hz), again because of bond polarity and space confinement. A three-orbital contribution involving these LMOs and the core LMO is also negative (−132 Hz, Table 1) so that the FC term is dominated by the positive bond LMO contribution, which is substantially reduced by lone pair LMO contributions. Taking all one- and two-orbital terms together a positive FC term results (355 Hz, Table 1), the sign of which is confirmed by the total FC spin polarization density distribution being negative at H and positive at F (Fig. 6).

By analyzing the one-bond FC term of ^1J(F,H), a basic understanding of the FC coupling mechanism for all one bond SSCCs of the type ^1J(X,H) and also ^1J(X,Y) with X and Y being any element of the periodic table is gained. It turns out that (i) the node patterns are the same for all zeroth order XH bond LMOs and (ii) also for all zeroth order lone pair (X) LMOs in any XH_n molecule. (iii) The same holds for the first order LMOs so that (iv) all one- and two-orbital FC contributions to ^1K(X,H) have the same sign as found for FH. (v) This means that the relative size of bond and lone pair LMOs determines the magnitude and the sign of the FC term in one-bond XH coupling constants. The relative size of the various LMO contributions depends in turn on the physicochemical properties of X, especially its electronegativity and polarizability. For example, it is easy to predict that the negative lone pair FC contributions should increase within a group (X = F to I) because of increasing lone-pair density at the position of the proton, which should be more pronounced than the increase of bonding electron pair density at H. Accordingly, the exponential increase of the ^{1}FC(X,H) term within a group of the periodic table[61,117] will be reduced and finally inverted with increasing number of valence electron lone pairs for molecules XH_n. This is of course relevant in connection with the observed dependence of total ^1K(X,H) values on the atomic number[117] where however other Ramsey terms will also play a role.[61]

Extension of the observations and predictions made for one-bond XH SSCCs to one-bond XY SSCCs is straightforward where however it has to be considered that the two- and three-orbital contributions play a larger role. Geminal, vicinal, and long range FC coupling mechanisms can be analyzed in a similar way.[62,66,68] In this connection a differentiation between through-bond and through-space coupling mechanisms becomes important.

4.4.2 The spin dipole (SD) coupling mechanism. There are some essential differences between the FC and the SD coupling mechanisms. Responding (perturbing) nucleus and the electron system interact in the latter case nonlocally. The perturbing nuclear moment of (B) generates a dipole field that is monitored by the quadrupolar potential residing at the responding nucleus (A). Hence, the SD term is contrary to the FC term in being orientation dependent. For the purpose of determining the isotropic SD term, one has to calculate the diagonal elements of the SD tensor, which are obtained when the quadrupole potentials represented by operators $\hat{B}_A^{\mathrm{SD}}$ and $\hat{B}_B^{\mathrm{SD}}$ adopt the same orientation. If they have different orientations, the off-diagonal elements of the SD tensor will be obtained, which do not enter the isotropic SD term.

The diagonal components of the SD tensor, $K_{AB,ii}^{\mathrm{SD}}$ ($\kappa = x, y, z$) are evaluated from six subcomponents $K_{AB,(\kappa\lambda)}^{\mathrm{SD}}$:[63]

$$K_{AB,\kappa\kappa}^{\mathrm{SD}} = \sum_{\lambda} K_{AB,(\kappa\lambda)}^{\mathrm{SD}} \tag{35a}$$

$$K_{AB,(\kappa\lambda)}^{\mathrm{SD}} = 4\sum_{k}^{\mathrm{occ}} \left\langle \phi_k^{(0)} | \left(\hat{\boldsymbol{B}}_{A,(\kappa\lambda)}^{\mathrm{SD}} \right) | \phi_{k,(\kappa\lambda)}^{(B),\mathrm{SD}} \right\rangle. \tag{35b}$$

where the symbol ($\kappa\lambda$) = (xx), (yy), (zz), (xy), (xz) or (yz) specifies the orientation of the spin moment of the perturbing nucleus (first index) and the component of the associated dipole field (second index). Hence, for each SD orbital contribution these six subcomponents have to be calculated to obtain the three diagonal components and finally the isotropic value of SD. This holds also for the SD spin polarization density and its orbital contributions

$$m_{(\kappa\lambda)}^{(B),\mathrm{SD}}(\boldsymbol{r}) = 4\sum_{k}^{\mathrm{occ}} \phi_k^{(0)}(\boldsymbol{r}) \phi_{k,(\kappa\lambda)}^{(B),\mathrm{SD}}(\boldsymbol{r}) \tag{36}$$

with

$$\phi_{k,(\kappa\lambda)}^{(B),\mathrm{SD}} = \sum_{a} \frac{\langle \phi_a^{(0)} | F_{(\kappa\lambda)}^{(B),\mathrm{SD}} | \phi_k^{(0)} \rangle}{\varepsilon_a - \varepsilon_k} | \phi_a^{(0)} \rangle \tag{37}$$

and

$$\hat{F}_{(\kappa\lambda)}^{(B),\mathrm{SD}} = \hat{B}_{(\kappa\lambda)}^{(B),\mathrm{SD}} + \tilde{F}_{(\kappa\lambda)}^{(B),\mathrm{SD}} \tag{38}$$

where space orbitals ϕ rather than spin orbitals Ψ have been used. At the responding nucleus (A), the SD spin polarization density distribution is weighted with the quadrupole potential $\hat{B}_{(\kappa,\lambda)}^{(A),\mathrm{SD}}$

$$\hat{B}_{(\kappa\lambda)}^{(A),\mathrm{SD}} = \alpha^2 \left(3\frac{x_{A,\kappa} x_{A,\lambda}}{r_A^5} - \frac{1}{r_A^3} \delta_{\kappa\lambda} \right) \tag{39}$$

to yield the six subcomponents of the SD energy density distribution.

$$\rho_{(\kappa\lambda)}^{(AB),\mathrm{SD}}(\boldsymbol{r}) = \hat{B}_{(\kappa\lambda)}^{(A),\mathrm{SD}} m_{(\kappa\lambda)}^{(B),\mathrm{SD}}(\boldsymbol{r}) \tag{40}$$

These can also be split into one- and two-orbital terms. Hence, the subcomponents of the SD term can be written in short form as

$$\begin{aligned} K_{AB,(\kappa\lambda)}^{\mathrm{SD}} &= \int \mathrm{d}^3 r\, \hat{B}_{(\kappa\lambda)}^{(A),\mathrm{SD}} m_{(\kappa\lambda)}^{(B),\mathrm{SD}}(\boldsymbol{r}) \\ &= \int \mathrm{d}^3 r \rho_{(\kappa\lambda)}^{(AB),\mathrm{SD}}(\boldsymbol{r}) \end{aligned} \tag{41a}$$

and the total isotropic SD term as

$$\begin{aligned} K_{AB}^{\mathrm{SD}} &= \frac{1}{3}\sum_{\kappa\lambda} K_{AB,(\kappa\lambda)}^{\mathrm{SD}} = \frac{1}{3}\sum_{\kappa\lambda} \int d^3 r \rho_{(\kappa\lambda)}^{(AB),\mathrm{SD}}(\boldsymbol{r}) \\ &= \int d^3 r \rho^{(AB),\mathrm{SD}}(\boldsymbol{r}) \end{aligned} \tag{42}$$

where $\rho_{(\kappa\lambda)}^{(AB),\mathrm{SD}}(\boldsymbol{r})$ is the total isotropic energy density distribution.

As can be seen from Table 1, the total SD term of ^1J(FH) is just −6 Hz because individual orbital contributions cancel each other largely. The σ LMOs make together a negative contribution of −37 Hz whereas the π lone pair orbitals lead to a positive contribution of 44 Hz. Magnitude and sign of these LMO contributions can be understood when considering the SD coupling mechanism.

Fig. 7a shows a contour line diagram of the calculated $m_{(zz)}^{(H),SD}$ subcomponent of the SD spin polarization density distribution (perturbing moment at the H nucleus in z direction; z-component of spin polarization) resulting from the σ bond and lone pair LMO. Fig. 7c gives the corresponding diagram for the (xx) subcomponent. The two spin polarization density distributions resemble each other apart from the opposite signature. The SD spin–spin coupling mechanism for the σ LMOs is, similarly to the FC coupling mechanism, dominated by excitations into the σ*(FH) bond orbital as is confirmed by Fig. 7b showing a contour line diagram of the first-order bond orbital for the (xx) subcomponent of the SD spin polarization density distribution. The first order bond LMOs for the SD(xx) and the FC term resemble each other where the latter has a larger s character at the H nucleus in response to the localized FC perturbation. The first order bond LMO for SD(xx) however possesses considerable p_z character at both F and H thus making an SD contribution for this LMO possible according to the following selection rules for p-orbitals:[63]

$$\hat{B}_{(xx)}^{(B),SD} : p_x \rightarrow p_x^*, p_y \rightarrow -p_y^*, p_z \rightarrow -p_z^* \quad (43a)$$

$$\hat{B}_{(yy)}^{(B),SD} : p_x \rightarrow -p_x^*, p_y \rightarrow p_y^*, p_z \rightarrow -p_z^* \quad (43b)$$

$$\hat{B}_{(zz)}^{(B),SD} : p_x \rightarrow -p_x^*, p_y \rightarrow -p_y^*, p_z \rightarrow p_z^* \quad (43c)$$

$$\hat{B}_{(xy)}^{(B),SD} : p_x \rightarrow p_y^*, p_y \rightarrow p_x^* \quad (43d)$$

$$\hat{B}_{(xz)}^{(B),SD} : p_x \rightarrow p_z^*, p_z \rightarrow p_x^* \quad (43e)$$

$$\hat{B}_{(yz)}^{(B),SD} : p_y \rightarrow p_z^*, p_z \rightarrow p_y^* \quad (43f)$$

where * denotes a higher lying unoccupied p-orbital.

The scheme in the lower part of Fig. 7 gives in a simplified way the form of the $m_{(zz)}^{(H),SD}$ subcomponent generated by the bond orbital (similar pictures apply to all one- and two-orbital terms involving σ LMOs). It resembles a double cone along the z-axis with a dominance of β spin density along the FH axis and a surplus of α spin density in the outer regions of the F atom perpendicular to the bond axis. The signatures of the quadrupole potential generated by the responding nucleus (shown in Fig. 7a and c by the encircled plus and minus signs) reveal that the corresponding SD energy density distributions are dominantly negative where one has to consider the weighting with a factor r_A^{-3}, *i.e.* only the SD spin polarization density close to the F nucleus makes a sizable contribution. The $SD_{(zz)}$ subcomponent due to the bond LMO contribution is −68 Hz (Fig. 7), which dominates the value of the diagonal element $SD_{(zz)}$ (66 Hz) of this LMO.

The π(F) lone pair orbitals participate in the SD coupling mechanism mainly by excitations into high-lying Rydberg p-orbitals with some FH antibonding π* character. The (xx), (yy), and (zz) subcomponents all make positive contributions to ^{1}SD(F,H) (2 × 40 and 53 Hz, respectively; see Fig. 8a). This can be explained in the same way as done for the σ LMOs.[63] Taking all orbital contributions together, the total isotropic SD energy density distribution of Fig. 8b results, in which the axially oriented negative contributions of the σ LMOs can be clearly distinguished from the positive contributions from the π(F) lone pair LMOs which fill a torus around the F nucleus

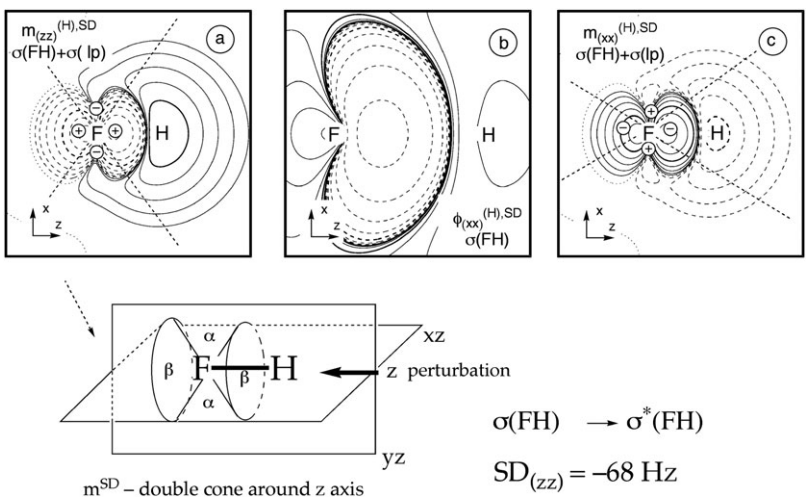

Fig. 7 Analysis of the SD term of the SSCC ^1J(F,H) calculated at the CP-DFT/BLYP(60:40) level of theory. (a) Contour line diagram of the SD spin polarization density distribution of the (zz) subcomponent for the contribution from the bond and σ lone-pair orbitals. (b) SD first-order bond orbital σ(FH) calculated for the (xx) subcomponent. (c) SD spin polarization density of the (xx) subcomponent for the contribution from the bond and σ lone-pair orbitals. Solid contour lines indicate positive values, dashed contour lines negative ones. The signature of the quadrupole potential at the responding nucleus F is indicated in sections (a) and (c). The drawing in the lower part gives schematically the double cone of the spin polarization density oriented along the bond axis (z-direction) as caused by the bond orbital.

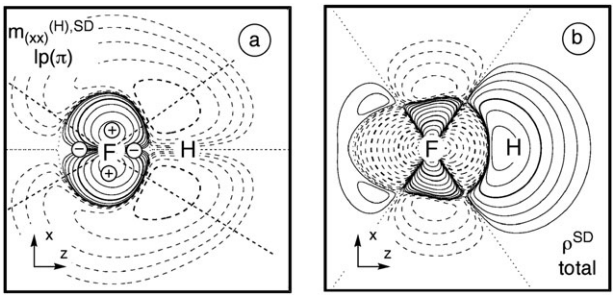

Fig. 8 Analysis of the SD term of the SSCC ^1J(F,H) calculated at the CP-DFT/BLYP(60:40) level of theory. (a) Contour line diagram of the SD spin polarization density distribution of the (*xx*) subcomponent for the contribution arising from the lone pair $p\pi_y$(F) orbital. (b) Total isotropic SD energy density distribution of the FH coupling constant given in form of a contour line diagram. Solid contour lines indicate positive values, dashed contour lines negative ones. The signature of the quadrupole potential at the responding nucleus F is indicated in section (a).

perpendicular to the axis. Because of the $r_A{}^{-3}$ weighting, the SD energy density is concentrated around the responding F nucleus. The regions of positive and negative SD energy density largely cancel so that a small negative isotropic SD term results for ^1J(F,H) (Table 1).

4.5 The spin–orbit terms

The second mechanism for the mediation of spin information between perturbing and responding nucleus is provided by the spin–orbit (SO) coupling mechanism (section 2.6). Despite the gauge ambiguity of the DSO and PSO terms, it is reasonable to ascribe them two different physical coupling processes: the DSO term reflects a Larmor precession of the electron system induced by the magnetic moment, *i.e.* an induction of orbital currents that are not present without the applied magnetic field. In contrast, the PSO mechanism describes a situation where orbital currents and resulting magnetic orbital moments are always (*i.e.* also in the absence of an external magnetic field) present but cancel each other as, *e.g.*, in the case of a closed p-shell. The applied magnetic field will modify (increase or decrease) these orbital currents and lift the mutual cancellation, resulting in a net orbital current and magnetic moment. This picture of para- and diamagnetic interactions is in line with the notion of para- and diamagnetism in classical electrodynamics.[1–5]

The DSO and PSO mechanisms require that different selection rules are fulfilled for the orbitals involved where these rules can be derived from the form of the perturbation operator. An easier way of comprehending the selection rules is based on the physical nature of the DSO and PSO coupling mechanisms. A Larmor precession can be induced in any orbital. Consequently, DSO coupling involves all orbitals of the molecule.

In contrast, the PSO term requires (i) previously existing orbital currents that (ii) must be modifiable by the external magnetic perturbation. Requirement (i) implies that PSO coupling can only take place if occupied orbitals with non-s character exist at the coupling nuclei. In most cases, the orbital currents are carried by *p* orbitals. Requirement (ii) implies that in addition low-lying virtual orbitals with non-s character must be present at the coupling nuclei. A more detailed analysis reveals[64] that the unoccupied orbitals must have the same angular momentum quantum number ℓ as the corresponding occupied orbital but be of a different type, *i.e.* differ with regard to the magnetic quantum number m_l, *e.g.*, $p_x \rightarrow p_y^*$ leads to a PSO contribution whereas $p_x \rightarrow p_x^*$ does not. Contrary to the ubiquitous DSO mechanism, the PSO mechanism will occur only if suitable occupied and virtual orbitals are available at the coupling nuclei. If PSO coupling is present it will mostly outweigh DSO coupling. Again, this is in line with para- and diamagnetism in classical electrodynamics.[1–5]

In analogy to the FC and SD terms, appropriate densities are useful to describe the coupling mechanism from a local point of view. These densities may be considered for the total SO coupling or for DSO and PSO separately. As in the case of the SD term, two kinds of densities are introduced to emphasize the separated roles of perturbing and responding nuclei: (i) the current densities $j_n^{(B),\mathrm{XSO}}(\boldsymbol{r})$ ($\kappa = x,y,z$, XSO = SO, DSO, PSO) describe the orbital current induced by the magnetic perturbation at atom *B* oriented in direction κ. (ii) The energy densities $\rho_\kappa^{(AB),\mathrm{XSO}}(\boldsymbol{r})$ specify the current density weighted with the vector potential from the nuclear magnetic moment at nucleus *A*, *i.e.*, the local contributions of the induced current density to the indirect spin–spin interaction energy. We will discuss the DSO and PSO terms for the FH molecule, making use of orbital contributions, current densities, and energy densities.

The spin–spin coupling between two nuclei is reciprocal, and an appropriate choice of the perturbing nucleus can simplify the analysis of the coupling mechanism. In the analysis of the SO terms, we will consider F as the perturbed nucleus and H as the responding one.

4.5.1 The diamagnetic spin–orbit (DSO) coupling mechanism. The DSO term is calculated utilizing the unperturbed (zeroth order) orbitals. Consequently, the DSO term comprises only one-orbital contributions, which we consider as direct Ramsey response terms. Calculated orbital contributions for the SD term of ^1J(F,H) are listed in Table 1.

The total DSO contribution amounts to just 0.2 Hz and is negligible as compared to the total ^1J(F,H) value. However, both the individual Cartesian components (maximally 90 Hz; not shown, see ref. 70) and the orbital contributions to the DSO term are non-negligible, which shows that the small total DSO contribution is due to a nearly complete mutual compensation between both Cartesian components and orbital contributions. As regards individual orbitals, the valence and lone-pair orbitals contribute between −12.8 Hz (bond orbital) and 9.5 Hz (π lone pair orbitals). Noteworthy is that the total contribution of the valence LMOs amounts to just 0.5 Hz, revealing that individual contributions from this group of LMOs largely cancel each other.

Magnitude and sign of the DSO orbital contributions can be explained with a theorem derived by us recently utilizing a multipole expansion of the charge densities and vector potentials around the perturbing nuclei:[58] *A spherical charge distribution centered at one of the coupling nuclei, e.g. the*

perturbing nucleus, does not contribute to the isotropic DSO term as long as it is restricted to a sphere with radius r(A,B). This theorem can be comprehended using a simple physical consideration: As mentioned in section 2, the direct spin–spin coupling between two nuclei vanishes in the isotropic average although the individual Cartesian components of the direct coupling tensor can be large. For a spherical charge distribution centered at the perturbing nucleus, the Larmor precession always takes place around an axis parallel to the magnetic nuclear moment and has always the same angular velocity. The resulting electronic magnetic moment has always the same magnitude and is always parallel to that of the perturbing nucleus. Consequently, DSO coupling mediated by such a charge distribution just acts as a slight amplification of direct spin–spin coupling. In the same way as the original direct spin–spin coupling, this amplification has non-vanishing individual Cartesian tensor components but a vanishing isotropic average.

In Fig. 9a and b, the DSO current density is shown for the perturbation oriented in x and z direction (now F being the perturbing nucleus to simplify the following discussion), respectively. The current densities indicate ring currents concentrated around the F nucleus, supporting the picture that the DSO coupling in FH acts as a slight amplification of the direct spin–spin coupling.

The core 1s(F) LMO leads to a very small DSO contribution (−0.3 Hz), which simply reflects the spherical symmetry of this orbital. For the valence LMOs, the inference can be reversed: the small total contribution of this orbital group indicates that (i) their total charge density is approximately spherical around the F nucleus and (ii) that the larger part of this spherical electron density distribution fits into a sphere with radius r being half the bond distance d(FH). Point (i) suggests that the FH bond is strongly polar so that the charge distribution around the F atom closely resembles that of a free F^- ion. In other words, the small total DSO value is a descriptor of the bond polarity of the FH molecule and by this also for the electronegativity difference between F and H. The value close to zero predicts large ionic character of the FH bond.

The signature of the valence and lone-pair contributions can be understood from another theorem formulated recently by us:[58] *The charge density inside the sphere around the diameter d(AB) of bond AB makes a negative contribution to the DSO term of J(A,B), the charge density outside this sphere, a positive contribution.* The DSO energy density distribution for J(F,H) is shown in Fig. 9c. The sphere that separates the region with negative DSO energy density (inside) from the region with positive DSO energy density (outside the sphere) is indicated (radius $r = 0.5\ d$(F,H)). This second theorem predicts the bond orbital contribution to be negative (−13 Hz: the bond orbital is situated mainly inside the reference sphere; Fig. 9c and Table 1) and the lone pair contributions to be positive (4, 5 and 5 Hz: the σ and π lone pair LMOs are situated mainly outside the reference sphere, Fig. 9c and Table 1). The total DSO term is small (typically $K < 0.1$ SI units) for the majority of all spin–spin couplings investigated. The question is whether there are indirect SSCCs, for which one should expect a large DSO term. The two theorems mentioned in this paragraph clarify that the DSO term scans charge anisotropy around each of the coupling nuclei. Thus, a large DSO contribution should be expected if the charge distribution around one of the coupling nuclei strongly deviates from isotropy as one may find this for certain transition metal atoms.

4.5.2 The paramagnetic spin–orbit (PSO) coupling mechanism. The total PSO term for ^1J(F,H) amounts to 204 Hz (Table 1) and makes, contrary to the DSO term, a substantial contribution to the total ^1J(F,H) SSCC. FH is insofar peculiar as the PSO term possesses the same order of magnitude as the FC term (355 Hz), whereas the total SSCC of hydrocarbons is often dominated by the FC term. The large weight of the PSO coupling in FH is due to three cooperating circumstances: (i) since the gyromagnetic ratios of the ^{19}F and ^{1}H nuclei are among the highest ones that have been observed,[76] the electronic spin-information transport is efficiently converted into large spin–spin coupling. (ii) The FC coupling mechanism is relatively weak in FH. In reduced units, FC(F,H) in FH is just about 50% of FC(C,H) in CH_4 and about 10% of FC(C,C) in C_2H_2. (iii) The electron structure in FH provides an intense PSO coupling mechanism between the F and H nuclei.

The large PSO term of ^1J(F,H) results almost exclusively from the lone-pair contributions. The π lone pair term is 202 Hz (Table 1), *i.e.* nearly equal to the total PSO term (204 Hz)

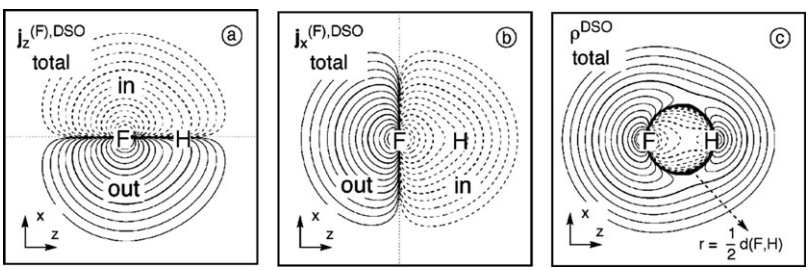

Fig. 9 Analysis of the DSO term of the SSCC ^1J(F,H) calculated at the CP-DFT/BLYP(60:40) level of theory.[70] Contrary to the contour line diagrams shown for the spin polarization terms, the F nucleus is chosen as the perturbing nucleus. The positions of F and H nuclei in the drawing plane are indicated by the element symbols. Contour levels chosen in geometric progression with a factor of $100^{1/5}$ between neighboring contour lines. Solid (dashed) lines refer to positive (negative) scalar densities or current densities out of (into) the drawing plane (indicated by "out" or "in"). Contour lines for 0.1 and 10 are printed in bold. All densities scaled by a factor of 10. (a) Total DSO current density distribution $\boldsymbol{j}^{(F),DSO}$ for the perturbation in z-direction. (b) Total DSO current density distribution $\boldsymbol{j}^{(F),DSO}$ for the perturbation in x-direction. (c) The total isotropic DSO energy density distribution ρ^{DSO}.

as the contributions from bond and σ lone pair LMO cancel each other largely (−54 and 47 Hz, respectively; Table 1). An analysis of the Cartesian components of the π lone pair contribution reveals that the *x* and *y* parts (318 Hz each) dominate over the *z* part (−23 Hz) and by this are the largest individual contributions to the total PSO term.

In view of the selection rules for a PSO contribution,[64] the *zz* component of the PSO coupling tensor is related to excitations of the kind $p_x \rightarrow p_y^*$ or $p_y \rightarrow p_x^*$, the *xx* component to excitations $p_y \rightarrow p_z^*$ or $p_z \rightarrow p_y^*$, and the *yy* component to excitations $p_x \rightarrow p_z$* or $p_z \rightarrow p_x$*.[64] Fig. 10a shows the first-order orbital for the π_y(F) lone pair LMO for the perturbation in *x*-direction, which possesses a distinct p_z character at the F nucleus because of the fact that it is dominated by the low-lying σ*(FH) orbital. The resulting orbital current (Fig. 10c) is a spatially extended ring current around the F atom with the ring axis in *x*-direction. This ring current has a large magnetic moment, giving rise to a strong induced magnetic field at the H atom and eventually to the observed large *x* PSO component for the π(F) lone pair LMOs.

The first-order π_y (F) lone pair LMO with perturbation in *z* direction (Fig. 10b) is dominated by a Rydberg $3p_x$ (F) orbital with a strong orthogonalization tail in the outer sphere of the F nucleus. The amplitude of this orbital is largest in the core region of F and relatively small otherwise, with a nodal sphere enveloping the F core region. The resulting orbital current (Fig. 10d) is characterized by two opposite ring currents (compare "in" and "out" signs in Fig. 10d), namely a relatively strong one in the core region of F and a weaker one in the region outside the core. The magnetic fields resulting from these ring currents largely cancel each other at the position of the H atom, which explains the relatively small *zz* PSO component resulting from the π(F) lone pair LMO (−23 Hz[70]). A similar observation can be made for the σ orbitals because lone pair and bond LMO lead to opposing ring currents, which again cancel each other largely.

The isotropic average of the total PSO energy density distributions is shown in Fig. 10e. The alternation of regions with positive and negative energy densities around the F nucleus results from the structure of the ring current (in-plane and out-of-plane currents make opposite contributions to the total PSO term), whereas the alteration of the energy density distribution around the H nucleus reflects the way the responding nucleus weights the orbital current density.

In subsection 4.5.1, we explained that, according to the DSO LMO contributions, the charge distribution around the F nucleus in FH resembles that of an F^- ion. DSO coupling from F to H just provides a slight amplification of the direct spin–spin coupling mechanism with substantial Cartesian components but a nearly vanishing isotropic average. One might expect that the same argumentation should apply for the PSO term and the isotropic PSO average should also become small. This is not the case for two reasons: (a) the PSO coupling probes not only the density but also the orbital structure close to the coupling nuclei. The orbital structure reflects anisotropy more sensitively than the electron density distribution. Therefore, there is a much closer resemblance between the DSO current densities for different orientations of the perturbing moment (see Fig. 9a and b) than for the corresponding PSO densities (see Fig. 10c and d). (b) The argumentation in section 4.5.1 assumed that the induced currents are restricted to the sphere centered at F with radius

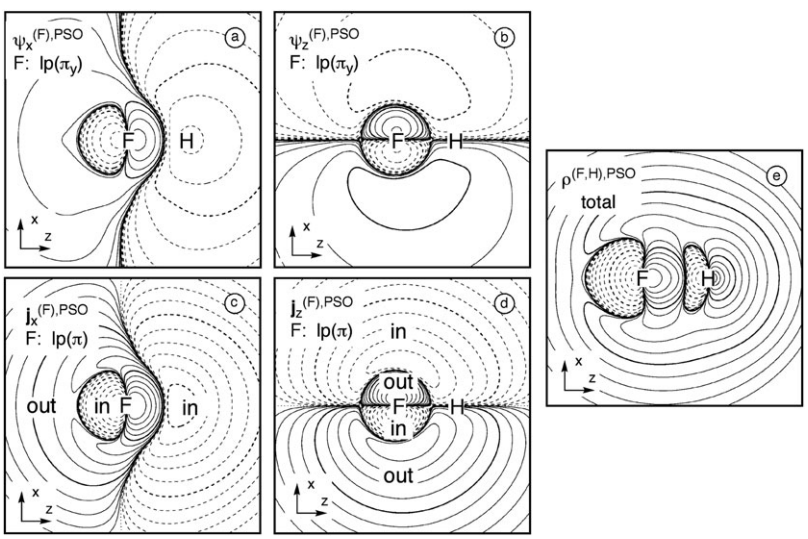

Fig. 10 Analysis of the PSO term of the SSCC ^1J(F,H) calculated at the CP-DFT/BLYP(60:40) level of theory.[70] Contrary to the contour line diagrams shown for the spin polarization terms, the F nucleus is chosen as the perturbing nucleus. The position of F and H nucleus in the drawing plane are indicated by the element symbols. Contour levels chosen in geometric progression with a factor of $100^{1/5}$ between neighboring contour lines. Solid (dashed) lines refer to positive (negative) scalar densities or current densities out of (into) the drawing plane (indicated by "out" or "in"). Contour lines for 0.1 and 10 are printed in bold. All densities scaled by a factor of 10. (a) PSO first-order π_y(F) lone pair LMO given for the perturbation in *x* direction. (b) PSO first-order π_y lone pair LMO given for the perturbation in *z* direction. (c) PSO current density distribution from the two (π) lone pair LMOs in the *xy*-plane for the perturbation in *x* direction, thus leading to a current in the *yz*-plane. (d) PSO current density distribution from the two π(F) lone pair LMOs in the *xy*-plane for the perturbation in *z*-direction, thus leading to a current in the *xy*-plane. (e) Total PSO energy density distribution for the responding nucleus H.

r(FH). The comparison of Fig. 9a and b on the one hand and 10c, 10d on the other hand reveals that this is true for the DSO current densities but not for the PSO current densities. The different behavior of the DSO and PSO terms underlines that these two terms probe different features of the electronic structure and thus provide complementary information.

Remarkably, the π(F) lone pair contribution of the PSO term contains a substantial portion (39%: 78 Hz, Table 1) of self-exchange repulsion. This term reflects that the exchange interaction between moving electrons is different from that of resting electrons with comparable orbital densities. It is also noteworthy that interactions between different orbitals play only a negligible role for the PSO term.

4.6 Comparison of J-OC-PSP to other analysis methods

Mechanistic analyses of the indirect spin–spin coupling are an active field of research, and a number of approaches have recently been suggested in the literature. One group of methods is to comprehend the coupling mechanism, in a similar spirit as the spin polarization, current, and energy densities we introduced in ref. 61–64. Malkina and Malkin[130] introduced a coupling energy density (CED), which was used among others to study through-bond and through-space contributions to ^{31}P–^{31}P coupling constants.[131] The usefulness of the CED is limited by the facts that (i) it covers only FC coupling and (ii) one has to calculate the perturbed wave function or orbitals of the molecule up to second order to determine the CED. The local approach developed by Soncini and Lazzeretti,[53] in contrast, covers all Ramsey terms and can be performed based on a conventional CP-DFT calculation. The current and energy densities defined in ref. 53 were used to study ^{3}J(H,H) in ethane[132] and the multipath coupling in propane and bicyclobutane.[133] The approach described by Soncini and Lazzeretti[53] is similar to ours[64] for the SO terms. The FC and SD terms, in contrast, are described with the help of current densities rather than spin polarization ones. Thus, the method of Soncini and Lazzeretti makes a formally uniform description of all four Ramsey terms possible. However, the description of the FC and SD coupling with a current density is physically less transparent than with a spin polarization density as done in J-**OC**-PSP.[61–63] As a complement to their original approach, Soncini and Lazzeretti described the steric-exchange part of the FC interaction with the help of a local exchange energy density.[134]

The NJC approach developed as NJC-1 by Contreras *et al.*[49] and later modified by Weinhold *et al.*[51,52] to yield NJC-2 allows an orbital analysis subsequent to an SSCC calculation at low computational cost and may therefore appear as an alternative to the J-**OC**-PSP approach. However, the NJC methods show a number of shortcomings: (i) Only NJC-1 is applicable to all Ramsey terms whereas NJC-2 is limited to the FC term. (ii) NJC focuses on the last step of the spin–spin coupling procedure, *i.e.* the interaction of the electron system with the responding nucleus. Thus, a balanced analysis of the whole spin–spin coupling is not possible. (iii) NJC is constrained to one-orbital contributions. It does not allow to determine orbital-interaction contributions. (iv) NJC is dependent on the use of NLMOs. As a consequence, NJC analyses are inevitably flawed by the problems that are connected with the use of NLMOs (see section 4.3). (v) NJC-2 requires that the magnetic perturbation is treated by finite-difference perturbation theory (FPT) rather than analytically. FPT does not provide an unambiguous definition of first-order orbitals in the same way as CP-DFT. Consequently, the definition of orbital contributions is not as transparent in NJC-2 as it is in a method based on CP-DFT. An alternative to NJC was suggested by Contreras *et al.*[50] In distinction to NJC, this approach provides a symmetric description of perturbed and responding nucleus. However, as it is based on an SOS approach, it gives no proper description of two-electron contributions. Recently, Contreras and co-workers studied the long-range coupling mechanism in substituted cubanes[135] and the influence of hyperconjugative effects on ^{1}J(C,H) couplings[136] based on conventional CP-DFT calculations of SSCC. To this purpose, a NBO analysis was performed for the molecules under investigation and the calculated SSCCs were correlated with the NBO occupation numbers. This approach allows in principle to settle one of the limitations of NJC, *viz*. its restriction to the FC term; however, it gives insight into the coupling mechanism in a rather indirect way only.

5. Concluding remarks and outlook

This article presents the work that has led to a better understanding and a detailed, quantum mechanically based analysis of the spin–spin coupling mechanism.[61–74] Our work is based on the reliable quantum mechanical calculation of SSCCs utilizing CP-DFT[58] and the J-**OC**-PSP analysis, which uses five different partitioning criteria considering (a) the physics of spin–spin coupling (Ramsey terms); (b) the spatial dependence of coupling (Cartesian components of SD, DSO, PSO terms); (c) the electron interactions that mediate the coupling (one- and two-electron contributions); (d) the role of the orbitals in the coupling process (orbital contributions); and (e) through-bond *versus* through-space or *through-tail* coupling (see section 5.2) (coupling *via* bond orbitals or orbital delocalization tails: Lewis or non-Lewis contributions). For the analysis, suitable sets of orbitals (LMOs, NBOs, *etc*.), spin polarization densities (FC and SD), orbital current densities (DSO and PSO), and Ramsey energy densities can be used. The Ramsey terms and their components have been reformulated to use either spin polarization densities or Ramsey energy densities thus facilitating the understanding of the coupling mechanism. The J-**OC**-PSP analysis developed by us fulfills the reciprocity, unconstrained applicability, physical justification, parallel processing, usefulness, additivity, and feasibility as well as all orbital criteria discussed in section 4.1. It correctly reflects the three-steps of the coupling mechanism and provides the physical and chemical insight into the nature of spin–spin coupling.

The J-**OC**-PSP method has been applied to a number of typical coupling situations between nuclei of the first two rows of the periodic table. These investigations have shown that measured SSCC, if combined with reliable calculations of their four Ramsey terms, provide a wealth of information on the electron structure of molecules, especially their bonding

situation. Important observations could be made utilizing the J-**OC**-PSP analysis. Here, just a few analysis results and observations should be mentioned.

5.1 General observations

The sign of a SSCC. It is possible to derive in certain cases rules for clarifying the sign of SSCCs. Based on the nodal structure of the zeroth order orbitals one can predict that of first order orbitals, FC and SD spin polarization densities as well as SD, DSO, and PSO energy density distributions so that the signature of orbital contributions for the Ramsey terms can be anticipated. In a number of cases it is also possible to identify the dominating terms so that the signature of the SSCC can be predicted. This is well-known for the case of ^{n}J(C,H) and ^{n}J(C,C) SSCCs in hydrocarbons,[15] which we could verify with the help of the J-**OC**-PSP analysis.[61,68] If hetero-atoms with lone pair orbitals are present, there is also the possibility of making predictions with regard to the signature of SSCC, at least in the case of one-bond SSCCs. However, in general it is not possible to reliably foresee the sign of a SSCC just by considering the nodal structure of zeroth and first order orbitals. The interplay of the various electronic effects in the coupling mechanism is too complex to make general predictions concerning the signature, which also has to be seen in connections with all the empirical or semiempirical attempts in this direction.

5.2 The FC coupling mechanism

Previous investigations focused on the FC coupling mechanism because this is the easiest to analyze and understand. Nevertheless, work with the J-**OC**-PSP method shows that a basic physical understanding of this mechanism was, despite the many investigations, dating decades ago, still missing.

The role of the bond orbital for one-bond FC coupling. The magnitude of the FC term of one-bond SSCC of the type ^{1}J(X,H) is strongly influenced by a positive bond LMO contribution, which increases within a group and a period (exceptions from the latter trend are explained in ref. 61). The J-**OC**-PSP analysis reveals that an efficient FC coupling mechanism requires both a large electronegativity (leading to a large contact spin density at the nucleus) and a large polarizability of X (leading to an effective transmission of spin polarization). The increase of the bond orbital term within a group results from an increase in the polarizability, and that within a period from an increased electronegativity.[61]

The role of the lone pair orbital for one-bond FC coupling. The lone pair and bond-lone pair LMO contributions to the FC term of one-bond SSCC of the type ^{1}J(X,H) are both negative, which is a result of the nodal properties of the lone pair LMO and can be rationalized with the help of the extended Dirac vector diagrams discussed in section 4.4.1. There is a similar increase of the absolute lone pair LMO contributions in dependence of the electronegativity and polarizability of X as found for the bond LMO contributions. If the number of lone pair LMOs increases within a period, it outweighs for higher atomic numbers the bond LMO contribution and leads to a negative FC term.[61]

Through-bond *versus* through-space coupling. Wilkens and co-workers have claimed using the NJC analysis[51] that the FC coupling mechanism for vicinal SSCCs such as ^{3}J(H,H) in ethane depends predominantly on through-bond coupling (the Lewis part of the coupling mechanism, see section 4.2). J-**OC**-PSP reveals that this claim is erroneous.[68] Spin–spin coupling is almost exclusively mediated *via* the tails of the CH bond orbitals in line with the rear-lobe mechanism of Barfield[36,37] or the first analysis of ^{3}J(H,H) in ethane by Karplus.[33–35] According to the J-**OC**-PSP results, the σ(CC) bond orbital in ethane has only a contribution of 0.1 Hz to the vicinal SSCC ^{3}J(H,H). The coupling mechanism in ethane takes an intermediate position between through-bond and through-space interaction, for which we have coined the term *through-tail interaction*.[68] We could explain the obscure findings of the NJC approach[51] by two of the insufficiencies of the NJC approach (see section 4.6): (a) NJC does not provide an analysis of all three steps of spin–spin coupling but only of the third step. This results in an incorrect separation between Lewis and non-Lewis contributions. (b) Since NJC is tied to NLMOs[68] and since the generation of NLMOs always leads to a mixing of orbitals, which contribute in a different way to the coupling mechanism, the NLMOs lead to a description of the spin–spin coupling mechanism, in which a separation of through-bond and through-space (through-tail) contributions is no longer possible.

The Karplus relationship and its dependence on substituent effects. The steric exchange two-orbital contribution of vicinal CH bonds and the corresponding bond orbital relaxation contributions (*i.e.* the individual contributions of the two CH bond orbitals) dominate the FC term of the vicinal SSCC ^{3}J(H,H) and govern also the form of the Karplus relationship between ^{3}FC (H,H) and dihedral angle τ. Since in all these terms the tails of the CH bond orbitals play the dominant role, one can consider coupling to be mediated by a through-tail mechanism (= through-space). The through-tail coupling vanishes at dihedral angles close to 90° and it is strongest at 0 and 180°. An electronegative substituent at a C atom of ethane leads to a contraction of the nearby CH bond orbital tails and thereby significantly reduces spin–spin coupling, whereas an electropositive substituent has the opposite effect (expansion of the tail; larger spin–spin coupling).

FC coupling *via* more than two bonds. The simplified picture that the spin–spin coupling mechanism follows the path given by the chemical bonds, *i.e.* a path of maximum electron density connections, is only true for the FC mechanism of one- or two-bond SSCCs in a limited way. Even for the FC term, through-space mechanisms are more important than is generally realized and they can become dominant for three- and more-bond SSCCs. This finding, obtained from the J-**OC**-PSP analysis of a large variety of SSCCs, is in line with Barfield's emphasis of rear-lobe interactions between orbitals as the major mechanism for through-space FC coupling over more than two bonds in hydrocarbons.[36,37]

The role of π-orbitals in the FC coupling mechanism. The π orbitals make a passive contribution to the FC coupling mechanism across a double bond adding 4.5 Hz to the FC

value (totally: 79.1 Hz[62]). This contribution can arise in two ways: either a π orbital gets spin polarized by an active orbital (spin-polarized directly by the perturbing nucleus) and causes in turn a change of that active orbital (echo mechanism); or an active orbital carries spin information to a π orbital, which forwards it to another spin orbital (transport mechanism). Either intra-atomic (intra-atomic Hund rule) or interatomic exchange interactions are responsible for the spin polarization mechanism.

Long-range H–H coupling in π systems. The J-**OC**-PSP analysis reveals that the long-range H–H coupling in polyenes is dominated by FC(π) contributions. The π system transports spin information efficiently over large distances along the bond framework where the mechanism is largely analogous to the *through-tail* mechanism found for the vicinal HH coupling in ethane, *i.e.* the π orbitals transfer spin information across the formal single bonds through their delocalization tails, which allow a formal single bond to be bridged by steric exchange interactions between adjacent π orbitals. This mechanism is so effective that ^{n}J(H,H) values should be observable up to $n = 17$.[66]

5.3 The SD coupling mechanism

The SD coupling mechanism requires occupied and unoccupied non-s orbitals. For CC bonds, the SD term results primarily from the (positive) one-orbital π contributions, which arise from π → π* excitations. Small contributions (either positive or negative) are also given by pseudo-π orbitals. The positive SD terms increase cubically with the bond order (or *p* character) of the CC bond.

SD-dominated long-range coupling. Long-range coupling in π systems should contain substantial SD contributions if the coupling nuclei are incorporated into the π system, *e.g.* for *J*(C,C) in unsaturated hydrocarbons or *J*(F,F) in the fluorinated analogues. The J-**OC**-PSP analysis shows that, under certain circumstances, for these couplings the SD term becomes the dominating contribution to the total coupling, which is relevant for quantum computing based on NMR spin–spin coupling.[128,129]

5.4 The DSO coupling mechanism

Since the DSO term is always rather small, the DSO coupling mechanism was so far the least interesting and therefore also the least investigated mechanism. However, the degree of smallness of the DSO term is a direct indicator of the anisotropy of the charge distribution centered at the coupling nuclei. A spherical charge distribution around one of two coupling nuclei *X* and *Y* makes only a little contribution to the DSO term of the SSCC. The bond and lone pair charge distributions at a nucleus *X* are normally nonspherical. However, their sum is approximately spherical at *X* so that the different orbital contributions cancel each other. Generally, those parts of the density distribution that are inside (outside) a sphere around the bond X–Y lead to negative (positive) contributions to the DSO term, thus explaining why the bond orbital contribution is negative, whereas the lone pair and external bond contributions are positive. In this way the DSO coupling mechanism is indicative of bond polarity and the electronegativity difference between two atoms X and Y.

5.5 The PSO coupling mechanism

The PSO coupling mechanism requires occupied as well as unoccupied non-s orbitals at the coupling nuclei. In the case of coupling between two first row atoms, the PSO mechanisms occur typically in π systems and systems containing heteroatoms with lone pairs. The J-**OC**-PSP analysis reveals that the isotropic PSO term is a consequence of several, sometimes contradicting, factors: (a) the existence of orbital pairs (occupied, unoccupied) with *p*π or *p*σ character and the right angular relationship, *i.e.*, *xy*, *xz* or *yz* for perturbation in the *z*-, *y*- or *x*-direction. The second component of the orbital pair is important for the nodal behavior of the first order orbital; (b) the induction of strong ring currents requires low excitation energies from the *x* to the *y* (*y* to *x*), the *x* to the *z* (*z* to *x*) or *y* to the *z* (*z* to *y*) component of the orbital pairs; (c) the orbital overlap between zeroth order and the first order orbital influences the magnitude of the ring current; (d) the nodal properties of zeroth and first order orbitals are decisive for whether a local ring current is increased or decreased. One can separate the various factors determining the PSO coupling mechanism if one considers its *xx*, *yy*, and *zz* components separately. On this basis it is easy to show why the isotropic PSO term is smaller for ^{1}J(C,C) in acetylene (negative σ(CC) LMO contribution partly cancels positive π(CC) LMO contribution) than the absolute isotropic PSO term for the same SSCC in ethene (negative σ(CC) LMO contribution and negative π(CC) LMO contribution). In the way the PSO coupling mechanism becomes clear it is possible to relate it to bond order, π-strength, electronegativity, and the magnetizability of a bond.[64,65]

5.6 Description of bonding with the help of spin–spin coupling

All results obtained so far with the J-**OC**-PSP analysis demonstrate clearly that there is no basis for the correlation of SSCCs such as ^{1}J(C,C) (or any other type of one-bond SSCC) with bond properties such as bond length, bond strength, bond-stretching frequencies, degree of hybridization (s-character), *etc*. The many previous, seemingly successful attempts in this direction were misleading because the number of data points was always too small and the selection of sample points biased. Nevertheless, there are some relationships, which are worth mentioning.

FC coupling. The FC term correlates linearly with the FC spin polarization density at the responding nucleus, which is insofar trivial as the FC term is determined, apart from a prefactor, directly from this spin density. Since the Fermi spin polarization density is in no simple way related to the s-density at the responding nucleus, it is obvious that relationships between FC term and s-density (degree of hybridization, s-character, *etc*.) can only hold for a limited number of similar bond situations.

Assessing the π character of a CC bond from the non-contact (NC) terms. The NC Ramsey terms provide a sensitive antenna for the π-character of a CC bond.[65,67] There is a cubic

dependence of the NC terms on increasing multiple bond character of a CC bond. The NC terms decrease from 1.2 Hz (normal CC single bond), to −0.4 (CC single bond with hyperconjugation), −1.5 (formal CC single bond in a conjugated system), −5.7 (aromatic CC bond), and −6 Hz (CC double bond), before they increase again to −3.9 (allene double bond), and 20 Hz (CC triple bonds). The cubic-type dependence of the NC term on the *p* character (bond order) of the CC bond results from the PSO term, which in turn adopts this form from the orbital contribution π(CC). It can be used to qualitatively assess the π-character of a CC bond.[65,67]

Nature of hydrogen bonds in biomacromolecules. According to the results of the J-**OC**-PSP analysis, spin–spin coupling across H bonds is based on two different effects: (I) an electrostatic field effect and (II) an orbital delocalization effect. Effects I and II show different geometry dependence. By an interplay of measurements and calculations, SSCC in biomacromolecules can be used to gain insight into the nature of the H-bonds.[71,72]

Multipath coupling. The J-**OC**-PSP analysis shows that the unusually large SSCC ^{2}J(C,C) between the bridge C atoms in bicyclo[1.1.1]pentane is dominated by through-bond interactions in the three C–C(H_2)–C paths (*multipath coupling*) between the coupling C atoms, with significant contribution arising from interactions between pairs of C–C(H_2)–C paths. For cyclopropane, which is another molecule with strong multipath coupling, the coupling mechanism reflects bonding features in the strongly strained ring: a large positive one-bond contribution (54 Hz: between 35 Hz for a CC single bond and 68 Hz for a CC double bond,[74]), reflecting the considerable π character of the CC bond in cyclopropane, a two-bond path contribution (geminal term: 10 Hz), a large negative through-space term corresponding to large overlap between CH bond orbitals (−27 Hz), and a substantial path-interaction term (−25 Hz). Together they lead to 12 Hz for ^{1}J(C,C) in line with measurements.[74]

5.7 Future use of the J-OC-PSP analysis

Despite the huge amount of literature on the nature of spin–spin coupling and its relationship to other molecular and especially bonding properties, this article shows that for a long time the true quantum mechanical nature of spin–spin coupling was not analyzed and understood in detail. Since the J-**OC**-PSP analysis provides for the first time a consistent and detailed analysis of all four Ramsey terms, within a relatively short time, the understanding of typical spin–spin coupling situations could be considerably advanced. Future work will focus on (a) the analysis of SSCC between heavier nuclei, especially those of transition metals,[137] (b) the search and design of SSCCs with special coupling features as, for example, a large SD term and (c) the development of relationships between SSCCs, their Ramsey terms and special electronic features. The present as well as the future work is/will be aimed at establishing SSCCs as sensitive antennae for the electronic structure of molecules.

Acknowledgements

DC thanks the University of the Pacific for supporting this work.

References

1 J. A. Pople, W. G. Schneider and H. J. Berstein, *High Resolution Nuclear Magnetic Resonance*, McGraw-Hill Book Co., New York, 1959.
2 J. W. Emsley, J. Feeney and L. H. Sutcliffe, *High Resolution Nuclear Magnetic Resonance Spectroscopy*, Pergamon Press, Oxford, 1968, vol. 1–2.
3 H. Günther, *NMR Spectroscopy—An Introduction*, John Wiley, New York, 1980.
4 E. D. Becker, *High Resolution NMR. Theory and Chemical Applications*, Academic Press, New York, 2nd edn, 1980.
5 R. K. Harris, *Nuclear Magnetic Resonance Spectroscopy*, Longman, Harlow, 1986.
6 E. Breitmeier and W. Voelter, *Carbon-13 NMR Spectroscopy*, VCH Publishers, New York, 3rd edn, 1987.
7 H.-O. Kalinowski, S. Berger and S. Braun, *Carbon-13 NMR Spectroscopy*, Wiley, Chichester, 1988.
8 R. J. Abraham, J. Fisher and P. Loftus, *Introduction to NMR Spectroscopy*, Wiley, Chichester, 1988.
9 C. P. Slichter, *Principles of Magnetic Resonance*, Springer, New York, 1990.
10 H. Duddeck and W. Dietrich, *Structure Elucidation by Modern NMR. A workbook*, Springer-Verlag, New York, 2nd edn, 1992.
11 J. K. M. Sanders and B. K. Hunter, *Modern NMR Spectroscopy*, Oxford University Press, Oxford, 2nd edn, 1993.
12 E. Breitmeier, *Structure Elucidation by NMR in Organic Chemistry. A practical guide*, Wiley, West Sussex, 1993.
13 F. A. Bovey, *Nuclear Magnetic Resonance Spectroscopy*, Academic Press, 1995.
14 P. J. Hore, *Nuclear Magnetic Resonance*, Oxford University Press, Oxford, 1995.
15 *Encyclopedia of Nuclear Magnetic Resonance*, ed. D. M. Grant and R. K. Harris, Wiley, Chichester, UK, 1996, vol. 1–8.
16 L. Griffiths and J. D. Bright, *Magn. Reson. Chem.*, 2002, **40**, 623.
17 A. Williams, *Curr. Opin. Drug Discovery Dev.*, 2000, **3**, 298.
18 J. Meiler, W. Maier, M. Will and R. Meusinger, *J. Magn. Reson.*, 2002, **157**, 242.
19 W. Robien, in *NMR Data Correlation with Chemical Structure, in Encyclopedia of Computational Chemistry*, ed. P. v. R. Schleyer, N. L. Allinger, T. Clark, J. Gasteiger, P. A. Kollman, H. F. Schaefer and P. R. Schreiner, Wiley, Chichester, UK, vol. 3, p. 1845.
20 D. Cremer, L. Olsson, F. Reichel and E. Kraka, *Isr. J. Chem.*, 1993, **33**, 369.
21 C.-H. Ottosson, E. Kraka and D. Cremer, in *Theoretical and Computational Chemistry, Pauling's Legacy—Modern Modelling of the Chemical Bonding*, ed. Z. Maksic, Elsevier, Amsterdam, 1999, vol. 6, p. 231.
22 T. Helgaker, M. Jaszunski and K. Ruud, *Chem. Rev.*, 1998, **99**, 293.
23 W. Kutzelnigg, U. Fleischer and M. Schindler, in *NMR-Basic Principles and Progress*, Springer, Heidelberg, 1990, vol. 23, p. 165.
24 U. Fleischer, C. v. Wüllen and W. Kutzelnigg, in *NMR Chemical Shift Calculation: ab initio*, in *Encyclopedia of Computational Chemistry*, ed. P. v. R. Schleyer, N. L. Allinger, T. Clark, J. Gasteiger, P. A. Kollman, H. F. Schaefer and P. R. Schreiner, Wiley, Chichester, UK, vol. 3, 1827.
25 H. Fukui, *Prog. Nucl. Magn. Reson. Spectrosc.*, 1992, **21**, 106; H. Fukui, *Prog. Nucl. Magn. Reson. Spectrosc.*, 1993, **22**, 138.
26 *Modeling NMR Chemical Shifts: Gaining Insights into Structure and Environment*, ed. J. C. Facelli and A. C. de Dios, ACS Symp. Ser. 732, American Chemical Society, Washington, DC. 1999.
27 A. C. de Dios and C. J. Jameson, in *The NMR chemical shift: Insight into structure and environment*, in *Annual Reports on NMR Spectroscopy*, ed. G. A. Webb, Academic Press, London, 1994, vol. 29, p. 1.
28 J. Kowalewski, *Prog. Nucl. Magn. Reson. Spectrosc.*, 1977, **11**, 1.

29 J. Kowalewski, *Annu. Rep. NMR Spectrosc.*, 1982, **12**, 81.
30 R. H. Contreras and J. C. Facelli, *Annu. Rep. NMR Spectrosc.*, 1993, **27**, 255.
31 R. H. Contreras and J. E. Peralta, *Prog. Nucl. Magn. Reson. Spectrosc.*, 2000, **37**, 321.
32 R. H. Contreras, V. Barone, J. C. Facelli and J. E. Peralta, *Ann. Rep. NMR Spectrosc.*, 2003, **51**, 167.
33 M. Karplus and D. H. Anderson, *J. Chem. Phys.*, 1959, **30**, 6.
34 M. Karplus, *J. Chem. Phys.*, 1959, **30**, 11.
35 M. Karplus, *J. Am. Chem. Soc.*, 1963, **85**, 2870.
36 M. Barfield, S. A. Conn, J. L. Marshall and D. E. Miller, *J. Am. Chem. Soc.*, 1976, **29**, 6253.
37 M. Barfield and B. Chakrabarti, *Chem. Rev.*, 1969, **69**, 757.
38 J. M. Schulman, J. Ruggio and T. J. Venanzi, *J. Am. Chem. Soc.*, 1977, **99**, 2045.
39 J. M. Schulman and T. J. Venanzi, *J. Am. Chem. Soc.*, 1976, **98**, 4701.
40 R. M. Dickson and T. Ziegler, *J. Phys. Chem.*, 1996, **100**, 5286.
41 A. R. Engelmann, R. H. Contreras and J. C. Facelli, *Theor. Chim. Acta*, 1981, **59**, 17.
42 H. Fukui, T. Tsuji and K. Miura, *J. Am. Chem. Soc.*, 1981, **103**, 3652.
43 H. Fukui, K. Miura, K. Ohta and T. Tsuji, *J. Chem. Phys.*, 1982, **76**, 5169.
44 A. R. Engelmann, G. E. Scuseria and R. H. Contreras, *J. Magn. Reson.*, 1982, **50**, 21.
45 M. A. Natiello and R. H. Contreras, *Chem. Phys. Lett.*, 1984, **104**, 568.
46 A. C. Diz, C. G. Giribet, M. C. Ruiz de Azua and R. H. Contreras, *Int. J. Quantum Chem.*, 1990, **37**, 663.
47 C. N. Cavasotto, C. G. Giribet, M. C. Ruiz de Azua and R. H. Contreras, *J. Comput. Chem.*, 1991, **12**, 141.
48 R. H. Contreras, M. C. Ruiz de Azua, C. G. Giribet, G. A. Aucar and R. Lobayan de Bonczok, *J. Mol. Struct. (THEOCHEM)*, 1993, **284**, 249.
49 J. E. Peralta, R. H. Contreras and J. P. Snyder, *Chem. Commun.*, 2000, 2025.
50 A. L. Esteban, M. P. Galache, F. Mora, E. Diez, J. Casanueva, J. San Fabian, V. Barone, J. E. Peralta and R. H. Contreras, *J. Phys. Chem. A*, 2001, **105**, 5298.
51 S. J. Wilkens, W. M. Westler, J. L. Markley and F. Weinhold, *J. Am. Chem. Soc.*, 2001, **123**, 12026.
52 E. M. Sproviero and G. Burton, *J. Phys. Chem. A*, 2002, **106**, 7834.
53 A. Soncini and P. Lazzeretti, *J. Chem. Phys.*, 2003, **118**, 7165.
54 J. L. Marshall, L. G. Faehl and R. Kattner, *Org. Magn. Reson.*, 1979, **12**, 163.
55 R. H. Contreras and G. E. Scuseria, *Org. Magn. Reson.*, 1984, **22**, 441.
56 G. A. Aucar, M. C. Ruiz de Azua, C. G. Giribet and R. H. Contreras, *J. Mol. Struct. (THEOCHEM)*, 1990, **205**, 79.
57 G. A. Aucar, V. Zunino, M. B. Ferraro, C. G. Giribet, M. C. Ruiz de Azua and R. H. Contreras, *J. Mol. Struct. (THEOCHEM)*, 1990, **205**, 63.
58 V. Sychrovský, J. Gräfenstein and D. Cremer, *J. Chem. Phys.*, 2000, **113**, 3530.
59 T. Helgaker, M. Watson and N. C. Handy, *J. Chem. Phys.*, 2000, **113**, 9402.
60 V. Barone, J. E. Peralta, R. H. Contreras and J. P. Snyder, *J. Phys. Chem. A*, 2002, **106**, 5607.
61 A. Wu, J. Gräfenstein and D. Cremer, *J. Phys. Chem. A*, 2003, **107**, 7043.
62 J. Gräfenstein, T. Tuttle and D. Cremer, *J. Chem. Phys.*, 2004, **120**, 9952.
63 J. Gräfenstein and D. Cremer, *Chem. Phys. Lett.*, 2004, **387**, 415.
64 J. Gräfenstein and D. Cremer, *Chem. Phys. Lett.*, 2004, **383**, 332.
65 J. Gräfenstein, E. Kraka and D. Cremer, *J. Phys. Chem. A*, 2004, **108**, 4520.
66 J. Gräfenstein, T. Tuttle and D. Cremer, *Phys. Chem. Chem. Phys.*, 2005, **7**, 452.
67 D. Cremer, E. Kraka, A. Wu and W. Lüttke, *ChemPhysChem*, 2004, **5**, 349.
68 J. Gräfenstein and D. Cremer, *Magn. Reson. Chem.*, 2004, **42**, S138.
69 J. Gräfenstein and D. Cremer, *J. Chem. Phys.*, 2004, **121**, 12217.
70 J. Gräfenstein, T. Tuttle and D. Cremer, *J. Phys. Chem. A*, 2005, **109**, 2325.
71 T. Tuttle, E. Kraka, A. Wu and D. Cremer, *J. Am. Chem. Soc.*, 2004, **126**, 5093.
72 T. Tuttle, J. Gräfenstein, A. Wu, E. Kraka and D. Cremer, *J. Phys. Chem. B*, 2004, **108**, 1115.
73 T. Tuttle, J. Gräfenstein and D. Cremer, *Chem. Phys. Lett.*, 2004, **394**, 5.
74 A. Wu and D. Cremer, *Phys. Chem. Chem. Phys.*, 2003, **5**, 4541.
75 N. F. Ramsey, *Phys. Rev.*, 1953, **91**, 303.
76 R. K. Harris and B. E. Mann, *NMR and the Periodic Table*, Academic Press, 1978.
77 J. E. Wertz and J. R. Bolton, *Electron Spin Resonance, Elementary Theory and Practical Applications*, McGraw-Hill, New York, 1972.
78 P. Hohenberg and W. Kohn, *Phys. Rev.*, 1964, **136**, B864.
79 R. G. Parr and W. Yang, *International Series of Monographs on Chemistry 16: Density-Functional Theory of Atoms and Molecules*, Oxford University Press, New York, 1989.
80 W. Kohn and L. J. Sham, *Phys. Rev.*, 1965, **137**, A1697.
81 S. H. Vosko, L. Wilk and M. Nusair, *Can. J. Phys.*, 1980, **58**, 1200.
82 J. P. Perdew and X. Wang, *Phys. Rev. B*, 1992, **45**, 13244.
83 A. D. Becke, *Phys. Rev. A*, 1988, **38**, 3098.
84 C. Lee, W. Yang and R. P. Parr, *Phys. Rev. B*, 1988, **37**, 785.
85 A. D. Becke, *J. Chem. Phys.*, 1993, **98**, 5648.
86 D. Cremer, *Mol. Phys.*, 2001, **99**, 1899.
87 V. Polo, J. Gräfenstein, E. Kraka and D. Cremer, *Chem. Phys. Lett.*, 2002, **352**, 469.
88 V. Polo, J. Gräfenstein, E. Kraka and D. Cremer, *Theor. Chem. Acc.*, 2003, **109**, 22.
89 J. Gräfenstein, E. Kraka and D. Cremer, *J. Chem. Phys.*, 2004, **120**, 524.
90 P. Bouř and M. Budesinsky, *J. Chem. Phys.*, 1999, **110**, 2836.
91 G. Vignale and M. Rasolt, *Phys. Rev. B*, 1988, **37**, 10685.
92 A. M. Lee, N. C. Handy and S. M. Colwell, *J. Chem. Phys.*, 1995, **103**, 10095.
93 C. Altona, in *Encyclopedia of Nuclear Magnetic Resonance*, ed. D. M. Grant and R. K. Harris, Wiley, Chichester, UK, 1996, vols. 1–8, p. 4909.
94 C. A. G. Haasnoot, F. A. A. M. De Leeuw and C. Altona, *Tetrahedron*, 1980, **36**, 2783.
95 C. Perez, F. Löhr, H. Rüterjans and J. M. Schmidt, *J. Am. Chem. Soc.*, 2001, **123**, 7081.
96 A. Wu, D. Cremer, A. A. Auer and J. Gauss, *J. Phys. Chem. A*, 2002, **106**, 657.
97 A. Wu and D. Cremer, *Int. J. Mol. Sci.*, 2003, **4**, 159.
98 A. Wu and D. Cremer, *J. Phys. Chem. A*, 2003, **107**, 1797.
99 D. Cremer and J. A. Pople, *J. Am. Chem. Soc.*, 1975, **97**, 1354.
100 D. Cremer, *J. Phys. Chem.*, 1990, **94**, 5502.
101 D. Cremer and K. J. Szabo, in *Methods in Stereochemical Analysis, Conformational Behavior of Six-Membered Rings, Analysis, Dynamics, and Stereoelectronic Effects*, ed. E. Juaristi, VCH Publishers, Weinheim, 1995, p. 59.
102 K. Hirao, H. Nakatsuji and H. Kato, *J. Am. Chem. Soc.*, 1973, **95**, 31.
103 T. A. Holak, D. W. Aksnes and A. Sygula, *Org. Magn. Reson.*, 1983, **21**, 287.
104 (*a*) D. Cremer and H. Günther, *Liebigs Ann. Chem.*, 1972, **763**; (*b*) for a summary, see H. Günther, in *Encyclopedia of Nuclear Magnetic Resonance*, ed. D. M. Grant and R. K. Harris, Wiley, Chichester, UK, 1996, vol. 1–8, p. 4925.
105 N. Muller and D. E. Pritchard, *J. Chem. Phys.*, 1959, **31**, 786.
106 N. Muller and D. E. Pritchard, *J. Chem. Phys.*, 1959, **31**, 1471.
107 C. J. Jameson and H. S. Gutowsky, *J. Chem. Phys.*, 1969, **51**, 2790.
108 K. Frei and H. J. Bernstein, *J. Chem. Phys.*, 1963, **38**, 1216.
109 Z. B. Maksic, *Int. J. Quantum Chem.*, 1971, **5**, 301.
110 Z. B. Maksic, M. Eckert-Maksic and M. Randic, *Theor. Chim. Acta*, 191, **22**, 70.
111 M. Barfield, M. J. Collins, J. E. Gready, S. Sternhell and C. W. Tansey, *J. Am. Chem. Soc.*, 1989, **111**, 4285.
112 M. Barfield, M. J. Collins, J. E. Gready, P. M. Hatton, S. Sternhell and C. W. Transey, *Pure Appl. Chem.*, 1990, **62**, 463.

113 S. Berger and K. P. Zeller, *J. Org. Chem*., 1984, **49**, 3725.
114 M. A. Fox and D. Schultz, *J. Org. Chem*., 1988, **53**, 4386.
115 H. Benedict, I. G. Shenderovich, O. L. Malkina, V. G. Malkin, G. S. Denisov, N. S. Golubev and H. H. Limbach, *J. Am. Chem. Soc*., 2000, **122**, 1979.
116 W. D. Arnold, J. H. Mao, H. H. Sun and E. Oldfield, *J. Am. Chem. Soc*., 2000, **122**, 12164.
117 J. P. Desclaux and P. Pyykkö, *Chem. Phys. Lett*., 1974, **29**, 534.
118 A. E. Reed, L. A. Curtiss and F. Weinhold, *Chem. Rev*., 1988, **88**, 899.
119 E. Kraka, J. Gräfenstein, M. Filatov, Y. He, J. Gauss, A. Wu, V. Polo, L. Olsson, Z. Konkoli, Z. He and D. Cremer, *COLOGNE 2006*, University of the Pacific, Stockton CA, 2006.
120 S. F. Boys, *Rev. Mod. Phys*., 1960, **32**, 296.
121 S. Berger, S. Braun and H. O. Kalinowski, *NMR-Spektroskopie Von Nichtmetallen Band 4, 19F-NMR-Spektroskopie*, Thieme, New York, 1994.
122 R. D. Wigglesworth, W. T. Raynes, S. P. A. Sauer and J. Oddershede, *Mol. Phys*., 1998, **94**, 851.
123 M. J. T. Jordan, J. S.-S. Toh and J. E. Del Bene, *Chem. Phys. Lett*., 2001, **346**, 288.
124 J. E. Del Bene, M. J. T. Jordan, S. A. Perera and R. J. Bartlett, *J. Phys. Chem. A*, 2001, **105**, 8399.
125 M. C. Böhm, J. Schulte and R. Ramirez, *Chem. Phys. Lett*., 2000, **332**, 117.
126 P. O. Åstrand, K. Ruud, K. Mikkelsen and T. Helgaker, *J. Chem. Phys*., 1999, **110**, 9463.
127 T. A. Ruden, O. B. Lutnaes, T. Helgaker and K. Ruud, *J. Chem. Phys*., 2003, **118**, 9572.
128 J. Gräfenstein and D. Cremer, to be published. See also ref. 129.
129 P. F. Provasi, G. A. Aucar and S. P. A. Sauer, *J. Phys. Chem. A*, 2004, **108**, 5393.
130 O. L. Malkina and V. G. Malkin, *Angew. Chem., Int. Ed*., 2003, **42**, 4335.
131 M. Kaupp, A. Patrakov, R. Reviakine and O. Malkina, *Chem.–Eur. J*., 2005, **11**, 2773.
132 A. Soncini and P. Lazzeretti, *Chem. Phys. Lett*., 2005, **409**, 177.
133 A. Soncini and P. Lazzeretti, *ChemPhysChem*, 2006, **7**, 679.
134 A. Soncini and P. Lazzeretti, *J. Chem. Phys*., 2003, **119**, 1343.
135 R. H. Contreras, A. H. Esteban, E. Diez, E. W. Della, I. J. Lochert, F. P. dos Santos and C. F. Tomena, *J. Phys. Chem. A*, 2006, **110**, 4266.
136 R. H. Contreras, A. L. Esteban, E. Diez E, N. J. Head and E. W. Della, *Mol. Phys*., 2006, **104**, 485.
137 J. Gräfenstein and D. Cremer, to be published.

